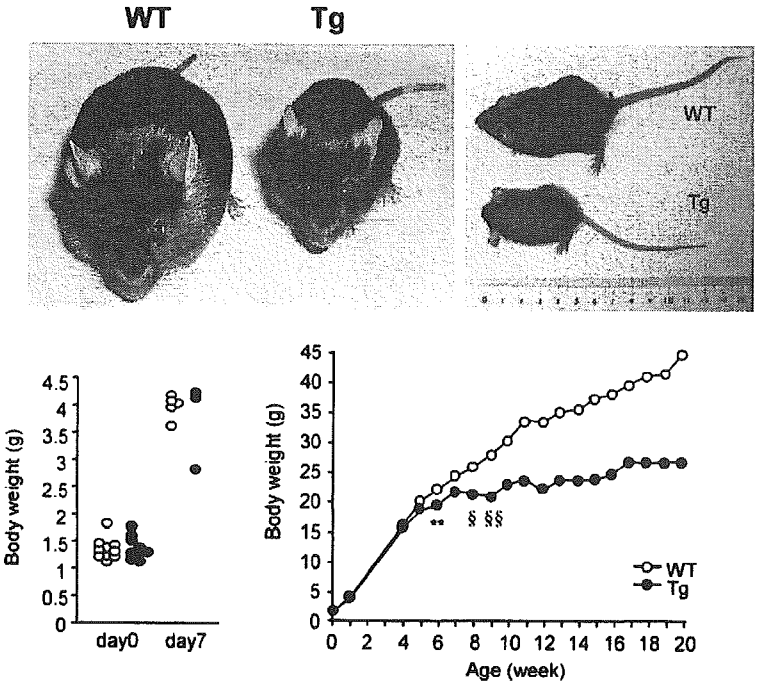

FIG. 4. Body weights of male mice (line Tg23). (Top) Photograph of male Tg mouse and control littermate (WT) at 12 weeks of age. (Bottom) Body weights of male WT (open circles) and Tg (solid circles) mice were similar to those of WT mice at days 0 and 7. The growth curve of male mice from day 0 to 20 weeks of age (n = 10) is shown. **, $P < 0.01$; at 6 weeks, §, $P < 0.005$; after 9 weeks, §§, $P < 0.001$.

markedly reduced, as were insulin content and mRNA levels. Since, as we previously have shown, the levels of β-cell-specific transcripts, such as GLUT2, glucokinase, PDX-1, and IAPP, are downregulated by hyperglycemia (33, 36, 37), normalization of insulin gene expression to another β-cell-specific gene would not be valid. The islet deficits are partly due to the depletion of β cells, but some of the reductions are direct effects of the overexpression of ICER. The insulin promoter luciferase assays showed that ICER directly repressed insulin gene transcription. In addition, as shown by electron microscopy insulin granules were remarkably decreased in individual β cells, thereby confirming the inhibitory effect of ICER on insulin expression. Thus, in this Tg model, diabetes resulted from a decreased number of β cells, further compounded by impaired insulin expression in individual β cells.

After birth, replication of preexisting β cells is the main means of expanding the β-cell population (24). Islets in late fetal life have an equal proportion of β and non-β cells, but after the perinatal burst of replication, the β cells comprise about 75% of the islet. This increase in proportion results from the discordance of proliferation between the β and non-β endocrine cells in the perinatal period. CREM and CREB have been reported to be involved in the regulation of cell proliferation and regeneration in the liver (8, 52). One effect may be through cyclin A, whose expression at S phase and association with cdc2 are required for cell proliferation (48, 56). The induction of the cyclin A gene is limited to a short period of the cell cycle during which the expression levels of phosphorylated CREM and CREB are high while that of ICER is low (9). Furthermore, a moderate amount of cyclin A is required for normal cell cycle progression, since the G_1/S transition is accelerated by cyclin A overexpression (49). Therefore, it is possible that overexpressed ICER had inhibitory effects on the cell cycle and its progression. Consistent with the ability of ICER to suppress cyclin A promoter activity (Fig. 1C), cyclin A mRNA and protein levels were markedly reduced in islets of Tg mice compared to WT mice, but not in acinar cells. Furthermore, using double immunostaining for insulin and Ki67, a marker for β-cell proliferation, we found few, if any, β cells in the replicative cycle at 7 days of age even though about 30% of the β cells of the WT mice were in the cell cycle. These results suggest that reduction of cyclin A expression by ICER may limit β-cell proliferation. In addition, the presence of singlets-doublets of insulin-positive cells scattered throughout the pancreas suggested that neogenesis was still occurring. No evidence of abnormally increased apoptosis was seen at this time, although it cannot be ruled out that there was increased apoptosis earlier, possibly in the fetal period. Therefore, decreased replication is the likely basis of depletion of β cells within Tg mouse islets.

During the preparation of this paper, a report on dominant-negative A-CREB Tg mice showed an increased apoptosis via IRS2 reduction in β cells, leading to a late-onset, mild diabetes (32). A-CREB is a dominant-negative inhibitor of CREB, constructed by replacing the CREB basic region with an acidic amphipathic protein sequence; it is only 82 amino acids long whereas the full-length CREB is 342 amino acids (1). These mice have normal blood glucose levels and islet architecture until 8 weeks of age, after which apoptosis leads to a decreased β-cell number and mild diabetes by 12 weeks of age. In contrast, our ICER mice developed early severe diabetes with markedly reduced insulin secretion and islet insulin content

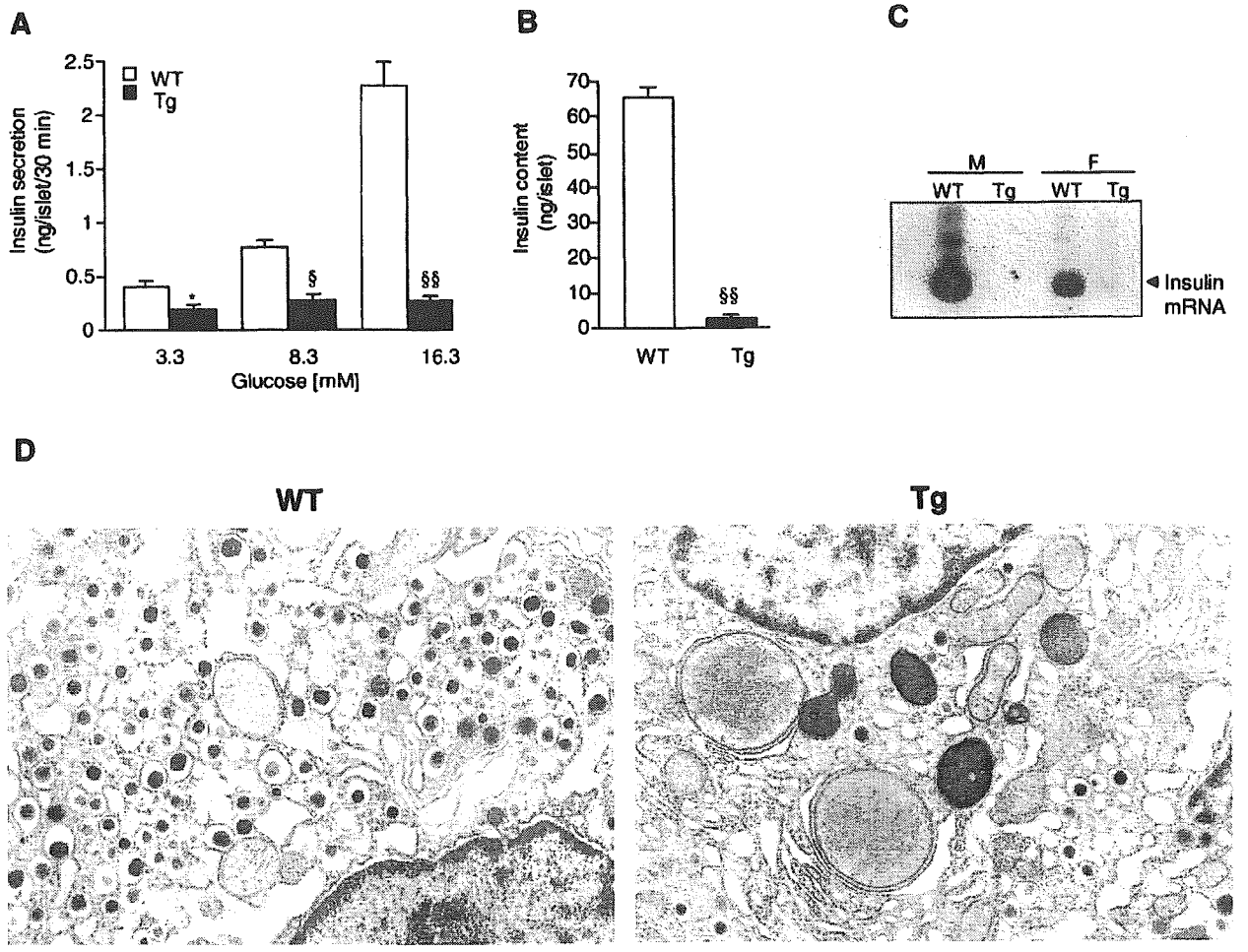

FIG. 5. Insulin secretion and β-cell morphology of isolated islets (line Tg23). (A and B) Glucose-stimulated insulin secretion (A) and insulin content (B) were examined using islets freshly isolated from 12-week-old male Tg (n = 5) and WT (n = 5) mice. These islets were matched for size. Three independent isolations and/or experiments were performed. *, $P < 0.05$; §, $P < 0.005$; §§, $P < 0.001$. (C) Northern blot analysis of insulin mRNA levels in male (M) or female (F) mice. Total islet RNA (20 μg) freshly extracted from isolated islets of 10-week-old Tg (n = 10) and WT (n = 10) mice was used. (D) β-cell morphology as shown by electron microscopy at 36 weeks of age. Control β cells (left) contained numerous mature insulin secretory granules surrounded by clear wide halos. In contrast, there were markedly fewer insulin secretory granules within β cells in Tg mice (right).

and a reduced number of β cells. What is striking about our Tg mouse model was that the animals became hyperglycemic by 7 days of age, and islet morphology was stable with marked reduction of β cells from an early age. The stability of islet morphology is more consistent with an impaired proliferation than with increased apoptosis. With increased apoptosis and no compensatory increase in replication, there should be a steady decline in the proportion of β cells in the islets, yet this is not what we observed. In fact apoptosis, as shown by TUNEL staining, was not increased at this early age, and β-cell replication, which is normally active at this age, was severely decreased in our ICER Tg mice. Thus, the reduced number of β cells in our Tg mice is more consistent with a decreased proliferation than with increased apoptosis.

The discrepancy between our data and those for A-CREB Tg mice must be based on the different mechanisms of inhibition of ICER and A-CREB. ICER has a strong binding ability (29), and a small amount of ICER efficiently competes and prevents binding of activators. While ICER homodimer formation is more favored than that of the heterodimer ICER-CREM activator, ICER also forms heterodimers with all CREM proteins and CREB, generating nonactivating dimers (41). Thus, ICER occupies DNA-binding sites (CREs) as either a homodimer or an inactive heterodimer and blocks promoter activity by preventing the binding of other members of the basic leucine zipper (B-Zip) proteins, such as CREB, CREM, ATF, Jun, and Fos. In contrast, A-CREB as a homodimer is less stable than a CREB homodimer but selectively forms with CREB a very stable heterodimer that is 3,300-fold more stable than a CREB homodimer (1). However, A-CREB is unable to form heterodimers with other B-Zip proteins and so selectively prevents the binding of CREB to DNA (1).

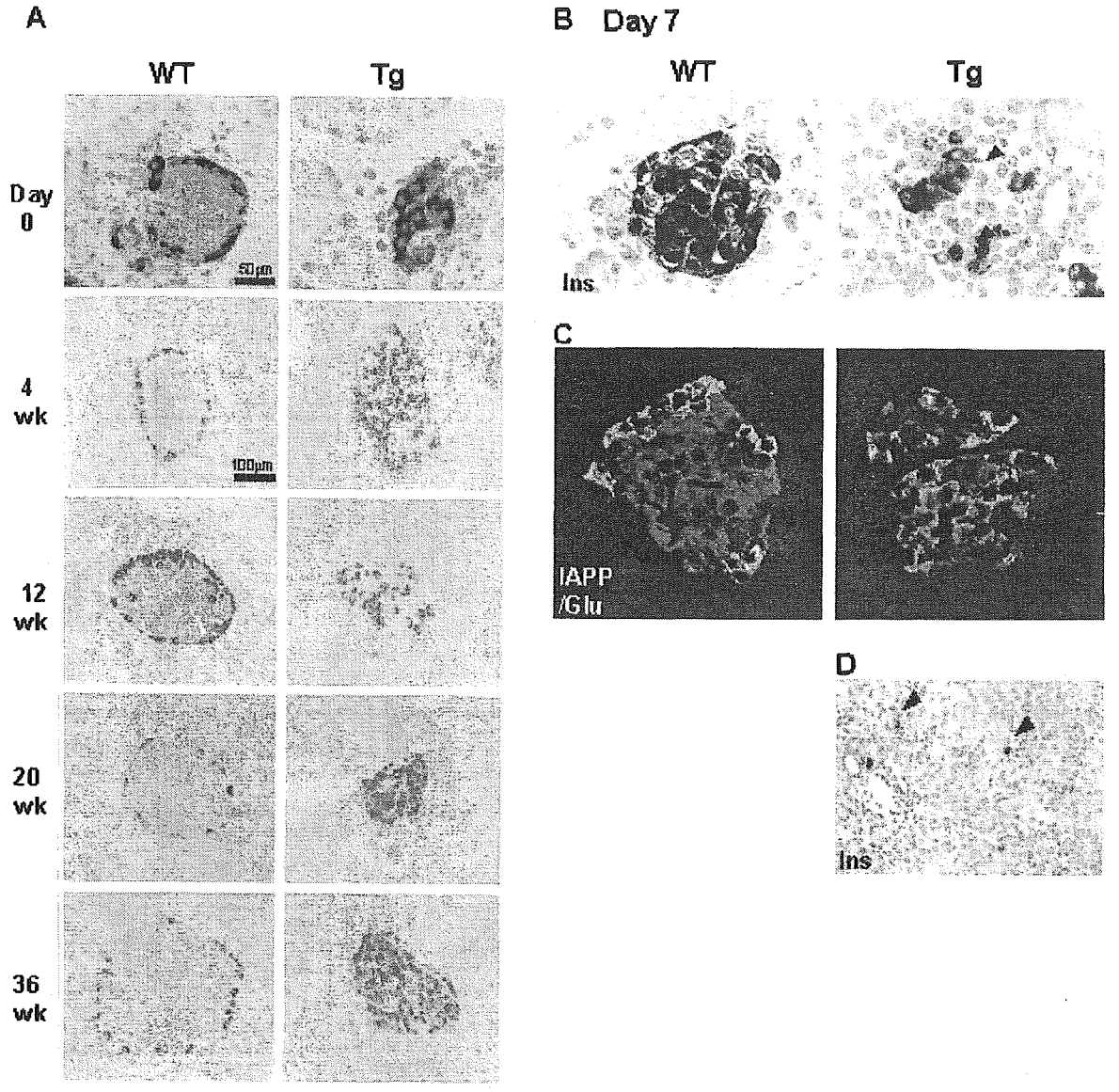

FIG. 6. Islet morphology (line Tg23). (A) Immunohistochemical staining of pancreatic sections from 0-day-old (nondiabetic condition) to 36-week-old (severe diabetes) mice with anti-insulin and antiglucagon antibodies. In Tg mice far fewer insulin-positive (pink) cells are present even at day 0, so the islets appear severely disorganized with a significantly increased proportion of glucagon-positive (red) cells, indicating that these changes result directly from the increased ICER Iγ and are not due secondarily to hyperglycemia. (B) Reduced insulin-positive cells in Tg mice (arrowhead) at 7 days. Additionally in the Tg mouse there is a marked variation in the amount of insulin per cell (degranulation) as shown by the insulin staining. (C) Dual staining of IAPP (red) as a β-cell marker and glucagon (green) was analyzed by confocal microscopy. (D) Scattered singlets-doublets of insulin-positive cells (arrowheads) in Tg mice. Magnification, ×1,000 (B and C) and ×400 (D).

Considering that other B-Zip proteins, such as ATF-2, ATF-3, ATF-4, Jun, and Fos, can form heterodimers with each other and bind to CRE to activate gene transcription (20, 22, 50), it is possible that these B-Zip proteins could function in CREB-independent signaling pathways or compensate for CREB function in CREB-dependent signaling pathways in the A-CREB Tg mice, as was observed with CREB-knockout mice (3, 26). Taken together, these different mechanisms of repression may account for the very different, but complementary, findings from the work of Jhala et al. (32).

In conclusion, we found that inhibition of CRE-binding activator function in pancreatic β cells by the repressor ICER Iγ suppresses insulin and cyclin A expression. The early severe diabetes in this model probably results from both the depleted insulin expression in individual β cells and the decreased number of β cells resulting from their impaired proliferation. Dynamic changes in ICER Iγ, from transient induction to its own suppression, are likely to be important for pancreatic β-cell physiology both directly by regulation of gene expression and indirectly by regulation of β-cell mass.

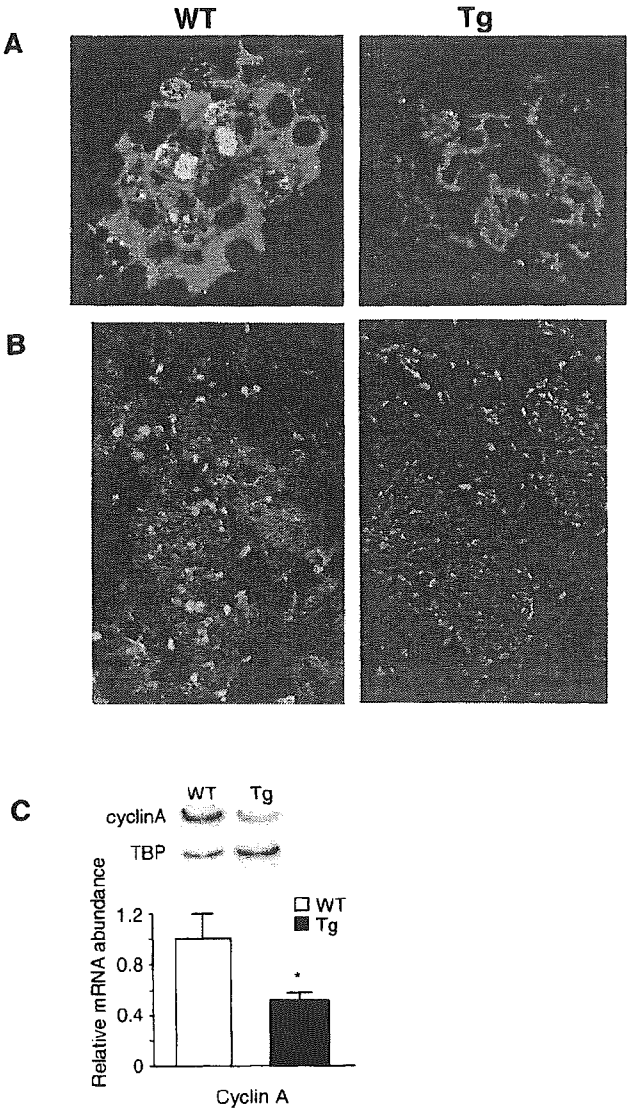

FIG. 7. Cyclin A expression and proliferation in islets at day 7 of age (line Tg23). (A) Dual staining of Ki67 (green) as a marker of cell proliferation and insulin (red) was analyzed by confocal microscopy. Ki67 was detected in 30% of the nuclei of β cells in WT mice but in few nuclei, if any, in Tg mice. (B) At day 7, normally a time of active cell proliferation, cyclin A protein was detected in most of the nuclei in islets in WT mice but in only a few islets of Tg mice. Magnification, ×1,000 (A) and ×400 (B). (C) Cyclin A mRNA level determined by semiquantitative PCR with islet cDNA is greatly reduced in Tg mouse islets. TBP, TATA-binding protein. *, $P < 0.05$.

ACKNOWLEDGMENTS

We thank Kinichiro Oda (Science University of Tokyo, Chiba, Japan) and Arata Takeuchi (Chiba University, Chiba, Japan) for providing the rat cyclin A promoter plasmid, Marina Schorpp-Kistner (Deutsches Krebsforschungszentrum, Heidelberg, Germany) for providing the mouse cyclin A promoter plasmid, and Joel. F. Habener (Massachusetts General Hospital, Howard Hughes Medical Institute, Boston, Mass.) for providing S4-CREM antibody. We thank Gordon C. Weir (Joslin Diabetes Center) and Shunsuke Ishii (Riken Tsukuba Institute, Japan) for critical reading of the manuscript and Hirofumi Noguchi and Rafael Nesher (Joslin Diabetes Center; Hebrew University Hadassah Medical Center, Jerusalem, Israel) for helpful discussions. We also thank Sarah Yasui and Shun Nawata for technical assistance, Haruyasu Kohda and Makio Fujioka for electron microscopy, Oogi Inada for frequent help with mouse care, Hiroshi Kanamori and Hidenori Arai for providing 7-day-old mouse pancreases, Chris Cahill for confocal microscopy, and Sonya Yokoff for fluorescent dual-color immunostaining.

This study was supported by in part by Grants-in-Aid for Scientific Research and for Creative Scientific Research (NP10NPO201) from the Ministry of Education, Culture, Sports, Science and Technology of Japan and by grants from the Research for the Future Program from the Japan Society for the Promotion of Science (JSPS-RFTF97I00201), the Joslin NIH DERC Advanced Microscopy Core, and the Diabetes and Wellness Research Foundation. A.I. is the recipient of a fellowship and grant from the Yamanouchi Foundation 2002 and from the Manpei Suzuki Diabetes Foundation 2002.

REFERENCES

1. **Ahn, S., M. Olive, S. Aggarwal, D. Krylov, D. D. Ginty, and C. Vinson.** 1998. A dominant-negative inhibitor of CREB reveals that it is a general mediator of stimulus-dependent transcription of *c-fos*. Mol. Cell. Biol. **18**:967–977.
2. **Andrecht, S., A. Kolbus, B. Hartenstein, P. Angel, and M. Schorpp-Kistner.** 2002. Cell cycle promoting activity of JunB through cyclin A activation. J. Biol. Chem. **277**:35961–35968.
3. **Bleckmann, S. C., J. A. Blendy, D. Rudolph, A. P. Monaghan, W. Schmid, and G. Schutz.** 2002. Activating transcription factor 1 and CREB are important for cell survival during early mouse development. Mol. Cell. Biol. **22**:1919–1925.
4. **Boam, D. S., A. R. Clark, and K. Docherty.** 1990. Positive and negative regulation of the human insulin gene by multiple *trans*-acting factors. J. Biol. Chem. **265**:8285–8296.
5. **Bodor, J., A. L. Spetz, J. L. Strominger, and J. F. Habener.** 1996. cAMP inducibility of transcriptional repressor ICER in developing and mature human T lymphocytes. Proc. Natl. Acad. Sci. USA **93**:3536–3541.
6. **Daniel, P. B., W. H. Walker, and J. F. Habener.** 1998. Cyclic AMP signaling and gene regulation. Annu. Rev. Nutr. **18**:353–383.
7. **De Cesare, D., and P. Sassone-Corsi.** 2000. Transcriptional regulation by cyclic AMP-responsive factors. Prog. Nucleic Acids Res. Mol. Biol. **64**:343–369.
8. **Della Fazia, M. A., G. Servillo, and P. Sassone-Corsi.** 1997. Cyclic AMP signaling and cellular proliferation: regulation of CREB and CREM. FEBS Lett. **410**:22–24.
9. **Desdouets, C., G. Matestic, C. A. Molina, N. S. Foulkes, P. Sassone-Corsi, C. Brechot, and J. Sobczak-Thepot.** 1995. Cell cycle regulation of cyclin A gene expression by the cyclic AMP-responsive transcription factors CREB and CREM. Mol. Cell. Biol. **15**:3301–3309.
10. **Docherty, K.** 1992. R. D. Lawrence Lecture. The regulation of insulin gene expression. Diabet. Med. **9**:792–798.
11. **Docherty, K., and A. R. Clark.** 1994. Nutrient regulation of insulin gene expression. FASEB J. **8**:20–27.
12. **Edlund, T., M. D. Walker, P. J. Barr, and W. J. Rutter.** 1985. Cell-specific expression of the rat insulin gene: evidence for role of two distinct 5′ flanking elements. Science **230**:912–916.
13. **Fimia, G. M., and P. Sassone-Corsi.** 2001. Cyclic AMP signalling. Cell Sci. **114**:1971–1972.
14. **Foulkes, N. S., E. Borrelli, and P. Sassone-Corsi.** 1991. CREM gene: use of alternative DNA-binding domains generates multiple antagonists of cAMP-induced transcription. Cell **64**:739–749.
15. **Foulkes, N. S., J. Borjigin, S. H. Snyder, and P. Sassone-Corsi.** 1996. Transcriptional control of circadian hormone synthesis via the CREM feedback loop. Proc. Natl. Acad. Sci. USA **93**:14140–14145.
16. **German, M., S. Ashcroft, K. Docherty, H. Edlund, T. Edlund, S. Goodison, H. Imura, G. Kennedy, O. Madsen, and D. Melloul.** 1995. The insulin gene promoter. A simplified nomenclature. Diabetes **44**:1002–1004.
17. **Gonzalez, G. A., and M. R. Montminy.** 1989. Cyclic AMP stimulates somatostatin gene transcription by phosphorylation of CREB at serine 133. Cell **59**:675–680.
18. **Gonzalez, G. A., K. Yamamoto, W. H. Fischer, K. Karr, P. Manzel, W. Biggs III, W. W. Vale, and M. R. Montminy.** 1989. A cluster of phosphorylation sites on the cyclic AMP-regulated nuclear factor CREB predicted by its sequence. Nature **337**:749–752.
19. **Goodison, S., S. Kenna, and S. J. Ashcroft.** 1992. Control of insulin gene expression by glucose. Biochem. J. **285**:563–568.
20. **Hai, T., and T. Curran.** 1991. Cross-family dimerization of transcription factors Fos/Jun and ATF/CREB alters DNA binding specificity. Proc. Natl. Acad. Sci. USA **88**:3720–3724.
21. **Hai, T. W., M. Horikoshi, R. G. Roeder, and M. R. Green.** 1988. Analysis of the role of the transcription factor ATF in the assembly of a functional preinitiation complex. Cell **54**:1043–1051.
22. **Hai, T. W., F. Liu, W. J. Coukos, and M. R. Green.** 1989. Transcription factor

ATF cDNA clones: an extensive family of leucine zipper proteins able to selectively form DNA-binding heterodimers. Genes Dev. **3**:2083–2090.
23. **Hamamoto, Y., Y. Tsuura, S. Fujimoto, M. Nagata, T. Takeda, E. Mukai, J. Fujita, Y. Yamada, and Y. Seino.** 2000. Recovery of function and mass of endogenous beta cells in streptozotocin-induced diabetic rats treated with islet transplantation. Biochem. Biophys. Res. Commun. **287**:104–109.
24. **Hellerstrom, C., I. Swenne, and A. Andersson.** 1988. An islet cell replication and diabetes, p. 141–170. *In* P. J. Lefebvre and D. G. Pipeleers (ed.), The pathology of the endocrine pancreas in diabetes. Springer-Verlag, Heidelberg, Germany.
25. **Hotta, M., F. Tashiro, H. Ikegami, H. Niwa, T. Ogihara, J. Yodoi, and J. Miyazaki.** 1998. Pancreatic β cell-specific expression of thioredoxin, antioxidative and antiapoptotic protein prevents autoimmune and streptozotocin-induced diabetes. Exp. Med. **188**:1445–1451.
26. **Hummler, E., T. J. Cole, J. A. Blendy, R. Ganss, A. Aguzzi, W. Schmid, F. Beermann, and G. Schutz.** 1994. Targeted mutation of the CREB gene: compensation within the CREB/ATF family of transcription factors. Proc. Natl. Acad. Sci. USA **91**:5647–5651.
27. **Hussain, M. A., P. B. Daniel, and J. F. Habener.** 2000. Glucagon stimulates expression of the inducible cAMP early repressor and suppresses insulin gene expression in pancreatic β-cells. Diabetes **49**:1681–1690.
28. **Inada, A., Y. Yamada, Y. Someya, A. Kubota, K. Yasuda, Y. Ihara, S. Kagimoto, A. Kuroe, K. Tsuda, and Y. Seino.** 1998. Transcriptional repressors are increased in pancreatic islets of type 2 diabetic rats. Biochem. Biophys. Res. Commun. **253**:712–718.
29. **Inada, A., Y. Someya, Y. Yamada, Y. Ihara, A. Kubota, N. Ban, R. Watanabe, K. Tsuda, and Y. Seino.** 1999. The cyclic AMP response element modulator family regulates the insulin gene transcription by interacting with transcription factor IID. J. Biol. Chem. **274**:21095–21103.
30. **Inagaki, N., T. Maekawa, T. Sudo, S. Ishii, Y. Seino, and H. Imura.** 1992. c-Jun represses the human insulin promoter activity that depends on multiple cAMP response elements. Proc. Natl. Acad. Sci. USA **89**:1045–1049.
31. **Ishii, S., T. Maekawa, T. Sudo, A. Sakurai, I. Yasuda, and A. Kishimoto.** 1990. Structure and function of the protein CRE-BP1: heterogeneity of the protein that binds to the cAMP-responsive element. Adv. Second Messenger Phosphoprot. Res. **24**:335–339.
32. **Jhala, U. S., G. Canettieri, R. A. Screaton, R. N. Kulkarni, S. Krajewski, J. Reed, J. Walker, X. Lin, M. White, and M. R. Montminy.** 2003. cAMP promotes pancreatic beta-cell survival via CREB-mediated induction of IRS2. Genes Dev. **17**:1575–1580.
33. **Jonas, J. C., A. Sharma, W. Hasenkamp, H. Ilkova, G. Patanè, R. Laybutt, S. Bonner-Weir, and G. C. Weir.** 1999. Chronic hyperglycemia triggers loss of pancreatic β cell differentiation in an animal model of diabetes. J. Biol. Chem. **274**:14112–14121.
34. **Knepel, W., J. Chafitz, and J. F. Habener.** 1990. Transcriptional activation of the rat glucagon gene by the cyclic AMP-responsive element in pancreatic islet cells. Mol. Cell. Biol. **10**:6799–6804.
35. **Krueger, D. A., D. Mao, E. A. Warner, and D. R. Dowd.** 1999. Functional analysis of the mouse ICER (inducible cAMP early repressor) promoter: evidence for a protein that blocks calcium responsiveness of the CAREs (cAMP autoregulatory elements). Mol. Endocrinol. **13**:1207–1217.
36. **Laybutt, D. R., M. Glandt, G. Xu, Y. B. Ahn, N. Trivedi, S. Bonner-Weir, and G. C. Weir.** 2003. Critical reduction in β-cell mass results in two distinct outcomes over time. J. Biol. Chem. **278**:2997–3005.
37. **Laybutt, D. R., A. Sharma, D. C. Sgroi, J. Gaudet, S. Bonner-Weir, and G. C. Weir.** 2002. Genetic regulation of metabolic pathways in β-cells disrupted by hyperglycemia. J. Biol. Chem. **277**:10912–10921.
38. **Maekawa, T., H. Sakura, C. Kanei-Ishii, C. Sudo, T. Yoshimura, J. Fujisawa, M. Yoshida, and S. Ishii.** 1989. Leucine zipper structure of the protein CRE-BP1 binding to the cyclic AMP response element in brain. EMBO J. **8**:2023–2028.
39. **Mao, D., E. A. Warner, S. A. Gurwitch, and D. R. Dowd.** 1998. Differential regulation and transcriptional control of immediate early gene expression in forskolin-treated WEHI7.2 thymoma cells. Mol. Endocrinol. **12**:492–503.
40. **Melloul, D., S. Marshak, and E. Cerasi.** 2002. Regulation of insulin gene transcription. Diabetologia **45**:309–326.
41. **Molina, C. A., N. S. Foulkes, E. Lalli, and P. Sassone-Corsi.** 1993. Inducibility and negative autoregulation of CREM: an alternative promoter directs the expression of ICER, an early response repressor. Cell **75**:875–886.
42. **Nielson, D. A., M. Welsh, M. J. Casadaban, and D. F. Steiner.** 1985. Control of insulin gene expression in pancreatic beta cells and in an insulin-producing cell line, RIN-5F cells. I. Effects of glucose and cyclic AMP on the transcription of insulin mRNA. J. Biol. Chem. **260**:13585–13589.
43. **Oetjen, E., T. Diedrich, A. Eggers, B. Eckert, and W. Knepel.** 1994. Distinct properties of the cAMP-responsive element of the rat insulin I gene. J. Biol. Chem. **269**:27036–27044.
44. **Philippe, J., and M. Missotten.** 1990. Functional characterization of a cAMP-responsive element of the rat insulin I gene. J. Biol. Chem. **265**:1465–1469.
45. **Philippe, J., E. Giordano, A. Gjinovci, and P. Meda.** 1992. Cyclic adenosine monophosphate prevents the glucocorticoid-mediated inhibition of insulin gene expression in rodent islet cells. J. Clin. Investig. **90**:2228–2233.
46. **Philippe, J., I. Pacheco, and P. Meda.** 1994. Insulin gene transcription is decreased rapidly by lowering glucose concentrations in rat islet cells. Diabetes **43**:523–528.
47. **Powers, A. C., F. Tedeschi, K. E. Wright, J. S. Chan, and J. F. Habener.** 1989. Somatostatin gene expression in pancreatic islet cells is directed by cell-specific DNA control elements and DNA-binding proteins. J. Biol. Chem. **264**:10048–10056.
48. **Riabowol, K., G. Draetta, L. Brizuela, D. Vandre, and D. Beach.** 1989. The cdc2 kinase is a nuclear protein that is essential for mitosis in mammalian cells. Cell **57**:393–401.
49. **Rosenberg, A., F. Zindy, F. L. Deist, H. Mouly, P. Metezeau, C. Brechot, and E. Lamas.** 1995. Overexpression of human cyclin A advances entry into S phase. Oncogene **10**:1501–1509.
50. **Ryseck, R. P., and R. Bravo.** 1991. c-JUN, JUN B, and JUN D differ in their binding affinities to AP-1 and CRE consensus sequences: effect of FOS proteins. Oncogene **4**:533–542.
51. **Sander, M., and M. S. German.** 1997. The beta cell transcription factors and development of the pancreas. J. Mol. Med. **75**:327–340.
52. **Servillo, G., M. A. Della Fazia, and P. Sassone-Corsi.** 1998. Transcription factor CREM coordinates the timing of hepatocyte proliferation in the regenerating liver. Genes Dev. **12**:3639–3643.
53. **Shimizu, M., Y. Nomura, H. Suzuki, E. Ichikawa, A. Takeuchi, M. Suzuki, M. Nakamura, T. Nakajima, and K. Oda.** 1998. Activation of the rat cyclin A promoter by ATF2 and Jun family members and its suppression by ATF4. Exp. Cell Res. **239**:93–103.
54. **Walker, M. D., T. Edlund, A. M. Boulet, and W. J. Rutter.** 1983. Cell-specific expression controlled by the 5′-flanking region of insulin and chymotrypsin genes. Nature **306**:557–561.
55. **Welsh, M., D. A. Nielsen, A. J. MacKrell, and D. F. Steiner.** 1985. Control of insulin gene expression in pancreatic beta cells and in an insulin-producing cell line, RIN-5F cells. II. Regulation of insulin mRNA stability. J. Biol. Chem. **260**:13590–13594.
56. **Yam, C. H., T. K. Fung, and R. Y. C. Poon.** 2000. Cyclin A in cell cycle control and cancer. Cell. Mol. Life Sci. **59**:1317–1326.

Y. Yamada [1]
Y. Seino [2]

Physiology of GIP – A Lesson from GIP Receptor Knockout Mice

Abstract

A much greater insulin response is observed after oral glucose load than after intravenous injection of glucose. The hormonal factor(s) implicated as transmitters of signals from the gut to pancreatic β-cells was referred to incretin; gastric inhibitory polypeptide or glucose-dependent insulinotropic polypeptide (GIP) is identified as one of the incretins. GIP exerts its effects by binding to its specific receptor, the GIP receptor, which is expressed in various tissues including pancreatic islets, adipose tissue, and brain. However, the physiological role of GIP has been generally thought to stimulate insulin secretion from pancreatic β-cells, and the other actions of GIP have received little attention. We have bred and characterized mice with a targeted mutation of the GIP receptor gene. From these studies, we now know that GIP not only mediates early insulin secretion by acting on pancreatic β-cells, but also links overnutrition to obesity by acting on adipocytes.

Key words
Diabetes · Obesity

Introduction

A much greater insulin response is observed after oral glucose load than after intravenous injection of glucose [1]. This effect is attributed to signals that arise from the gut following ingestion of glucose and stimulate insulin release from pancreatic β-cells. The hormonal factor(s) implicated as transmitters of signals from the gut to pancreatic β-cells are collectively referred to as incretins [2].

Two incretins have been identified – gastric inhibitory polypeptide or glucose-dependent insulinotropic polypeptide (GIP) and glucagon-like peptide 1 (GLP-1) (Fig. **1**). Both gut hormones are secreted in proportion to the quantity of meal ingested and potentiate insulin secretion. GIP was first isolated from porcine intestine on the basis of its ability to inhibit gastric acid secretion; this 42-amino-acid hormone is released from duodenal endocrine K cells after absorption of glucose or fat. Subsequent studies have revealed that GIP potentiates glucose-induced insulin secretion from pancreatic β-cells [3].

GIP exerts its effects by binding to its specific receptor, the GIP receptors, and activating adenylyl cyclase. We isolated the human GIP receptor (GIPR) gene and cDNA [4]. The GIPR has seven potential membrane-spanning domains, a feature characteristic of the vasoactive intestinal peptide (VIP)/glucagon/secretin receptor family of G protein-coupled receptors. The GIP receptor is expressed in various tissues including pancreatic islets, adi-

Affiliation
[1] Department of Diabetes and Clinical Nutrition, Kyoto University Graduate School of Medicine, Kyoto, Japan
[2] Kansai-Denryoku Hospital

Correspondence
Y. Yamada, M. D., Ph. D · Department of Diabetes and Clinical Nutrition, Kyoto University Graduate School of Medicine · 54 Shogoin-Kawahara-cho· Sakyo-ku · Kyoto 606-8507 · Japan · Phone: +81 (75) 751-3561 · Fax: +81 (75) 751-3677 · E-Mail: yamada@metab.kuhp.kyoto-u.ac.jp

Received 5 August 2004 · **Accepted after revision** 19 August 2004

Bibliography
Horm Metab Res 2004; 36: 771–774 © Georg Thieme Verlag KG Stuttgart · New York ·
DOI 10.1055/s-2004-826162 · ISSN 0018-5043

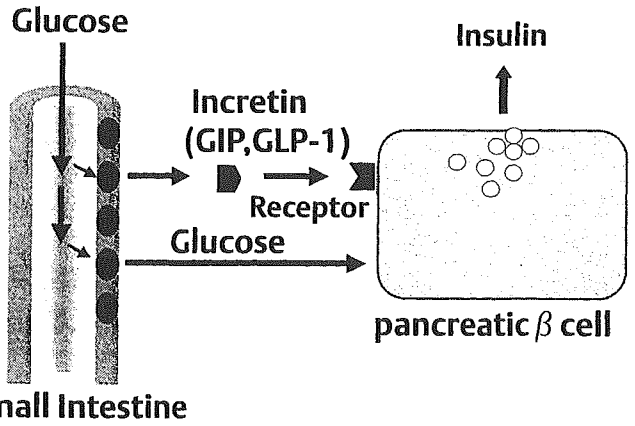

Fig. 1 Not only direct effect of glucose but also indirect effect of glucose via release of incretin such as GIP and GLP-1 stimulate insulin secretion from pancreatic β-cells.

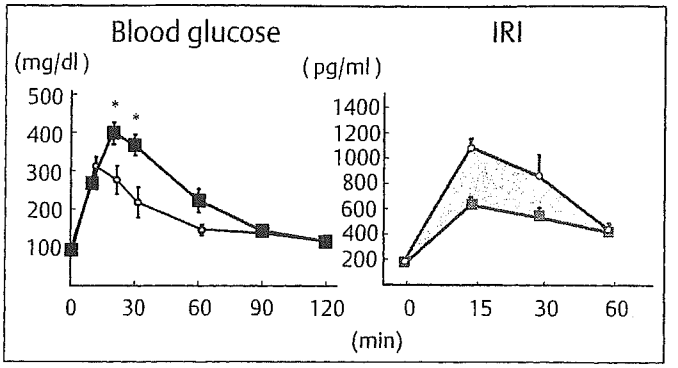

Fig. 2 Glucose tolerance test. Blood glucose levels (left) and plasma insulin levels (right) after oral glucose loading for the wild-type mice (open circle) and the GIP receptor KI mice (filled box). Estimated insulin secretion induced by GIP is shaded. From reference [6].

pose tissue, and brain [5]. However, the physiological role of GIP has generally been taken to be to stimulate insulin secretion from pancreatic β-cells; its other actions of GIP have received little attention.

We generated and characterized mice with a targeted mutation of the GIP receptor gene [6–11]. From these studies, we now know that GIP not only mediates early insulin secretion by acting on pancreatic β-cells, but also links overnutrition to obesity by acting on adipocytes.

GIP Receptor Knockout (KO) Mice

GIP receptor KO mice were generated as follows [6]. The 1.2-kb fragment containing exons 4 and 5 of the GIP receptor gene was replaced with a cassette containing the neomycin resistance gene. A negatively selectable marker gene, the herpes simplex virus thymidine kinase gene (HSV-TK), was placed external to the 3′ region of homology with the target locus. Embryonic stem (ES) cells were cultured without feeders in the presence of leukemia inhibitory factor, transfected with the targeting construct, and selected in the presence of G418 and gancyclovir. Colonies surviving positive and negative selection were isolated and screened to confirm that genuine homologous recombination had occurred on both sides of the gene. The chimeric mice were produced by microinjection of a targeted ES clone into blastocysts. Mice with the targeted allele were backcrossed to C57BL/6 mice before analysis of homozygous mice. The absence of GIP receptors was confirmed by batch-incubation studies using isolated pancreatic islets. GIP stimulated insulin secretion 2.9-fold from the islets of wild-type mice, but had no insulinotropic effect in the GIP receptor KO mice. The GIP receptor KO mice showed no gross abnormalities in general behavior or feeding or any histological abnormalities in pancreas, antrum, duodenum, or adrenal gland.

GIP as an Insulinotropic Peptide

In an intraperitoneal glucose tolerance test (IPGTT), blood glucose levels were not significantly different between wild-type or GIP receptor KO mice. However, in an oral glucose tolerance test (OGTT), the peak levels of blood glucose were delayed and significantly higher in GIP receptor KO mice compared to wild-type mice (Fig. **2**). Fasting insulin levels in the GIP receptor KO mice were identical to those in the wild-type mice. In contrast, at 15 min after glucose challenge, insulin levels in the GIP receptor KO mice were significantly lower than in the wild-type mice. The islets isolated from the GIP receptor KO mice secret insulin responding to glucose in a dose-dependent manner, and *in vitro* perfusions were carried out to confirm that insulin secretions stimulated by glucose in the wild-type and the GIP receptor KO mice were comparable [8]. Therefore, the decrease of insulin secretion after oral glucose challenge is not caused by impaired glucose-induced insulin secretion, but by disruption of the GIP enteroinsular axis. These results show the physiological role of GIP as an incretin, and further demonstrate that insulin secretion from the pancreatic β-cells is regulated not only by glucose but also by GIP, especially in the early phase after glucose ingestion (Fig. **2**).

Glucose-stimulated insulin secretion from pancreatic β-cells depends on glucose metabolism and electrical activity controlled by plasma membrane ion channels. The ATP-sensitive K (K_{ATP}) channel links glucose metabolism to membrane potentials. Recently, K_{ATP} channel-deficient mice were generated by genetic disruption of Kir6.2 [12]. The Kir6.2 KO mice still showed the insulin response after oral glucose loading *in vivo*, suggesting that elevation of intracellular cAMP concentration might induce insulin secretion even in the absence of the K_{ATP} channel. We generated mice that were deficient in both GIP receptor and K_{ATP} channel [11]. The GIP receptor and Kir6.2 double KO mice showed elevated blood glucose levels after oral glucose loading, and the insulin response was almost completely lost although insulin secretion from isolated islets was stimulated by GLP-1. Therefore, GIP is the major insulinotropic factor in the secretion of insulin in response to oral glucose loading in K_{ATP} channel-deficient mice.

Interaction of GIP and GLP-1 on Insulin Secretion

Perfusion and batch-incubation studies have demonstrated that the GIP receptor KO mice exhibit an increased insulin secretion in response to GLP-1 [8], which are consistent with the findings that GLP-1 produces higher intracellular cAMP levels in the GIP receptor KO mice than in the wild-type mice, implying that β-cell sensitivity to GLP-1 was increased. These results revealed upregulation of the compensatory mechanisms that take place within the enteroinsular axis.

We and the other group have generated and characterized the double incretin receptor KO mice with complete loss of both GIP and GLP-1 receptor action [9,10]. Double-incretin receptor KO mice showed impaired glucose tolerance and decreased insulin secretion after oral glucose loading. Furthermore, the glucose-lowering actions of dipeptidylpeptidase IV (DPP-IV) inhibitors were eliminated in the double-incretin receptor KO mice, suggesting that the GLP-1 and GIP signaling are the main targets for DPP-IV inhibitors, and that both incretins play a critical role in insulin release after meal ingestion.

GIP as an Obesity-promoting Factor

Plasma GIP concentrations have been reported as elevated in obese type 2 diabetic patients [13] and obese diabetic *ob/ob* mice [14], suggesting that GIP might induce obesity. Furthermore, functional GIP receptors was identified on adipocytes [15] and GIP has been shown to stimulate the synthesis and secretion of lipoprotein lipase in rat adipose tissue that hydrolyzes lipoprotein-associated triglycerides to produce free fatty acids available for local uptake [16]. However, the physiological significance of the anabolic effect of GIP was previously unclear. Using the GIP receptor KO mice, we have revealed that GIP directly links overnutrition to obesity [7].

The wild-type and the GIP receptor KO mice were fed either a control diet or a high-fat diet. On the control diet, which supplied 13% of calories as fat, 60% as carbohydrate and 27% as protein, with energy density of 3.57 kcal/g, body weights of the wild-type and the GIP receptor KO mice remained similar; on the high-fat diet, which supplied 45% of calories as fat, 35% as carbohydrate, and 20% as protein, with energy density of 3.57 kcal/g, the wild-type mice exhibited 35% body weight gain in the 50-week period. In contrast, there was no weight gain in the GIP receptor KO mice. Both visceral and subcutaneous fat mass was increased, and liver steatosis and hypertrophy of adipocytes was observed in high-fat-fed wild-type mice, but there was no such change in high-fat-fed GIP receptor KO mice. Insulin-tolerance test revealed that high-fat-fed wild-type mice had insulin resistance and that high-fat-fed GIP receptor KO mice remained as sensitive to insulin as controls, demonstrating that inhibition of the GIP signal prevents insulin resistance as well as obesity.

Obese *ob/ob* mice exhibit a marked increase in adipose tissue due to hyperphagia caused by mutation of the leptin gene. By crossbreeding the GIP receptor KO mice with *ob/ob* mice and generating double KO mice, we can show the role of the GIP signaling in adiposity, even in addition to leptin signaling.

The high-fat-fed GIP receptor KO mice showed the similar energy intake. We evaluated energy expenditure by measuring the respiratory quotient and oxygen consumption by indirect calorimetry. The respiratory quotient represents the proportion of fat and carbohydrate oxidation and the oxygen consumption represents the amount of energy combustion. After 3 weeks of high-fat feeding, the GIP receptor KO mice exhibited a significant reduction of respiratory quotient during the light phase, indicating that fat is utilized as preferred energy substrate in the GIP receptor KO mice and is not efficiently accumulated in adipocytes. After another 3 weeks on the high-fat diet, the wild-type mice consumed less oxygen than the GIP receptor KO mice during the light phase. These results clearly show that the resistance to obesity of the GIP receptor KO mice was due to higher energy expenditure rather than lower energy intake.

The GIP receptor is expressed in adipocytes and GIP stimulates cellular uptake of glucose and increases in heparin-releasable lipoprotein lipase (LPL) activity in 3T3-L1 adipocytes [7]. Therefore, GIP stimulates efficient uptake of nutrients into adipocytes; the loss of peripheral GIP actions in the GIP receptor KO mice may well have contributed to the increased fat oxidation without accumulating in adipocytes in these mice.

GIP has a physiological role on nutrient uptake into adipocytes, and is a key molecule linking overnutrition to obesity (Fig. **3**). Excessive fat intake induces hypersecretion of GIP. Hypersecretion of GIP increases nutrient uptake in the adipocytes that readily cause obesity and insulin resistance. Hyperinsulinemia could further increase nutrient uptake into the adipocytes, completing a vicious cycle of developing adiposity and insulin resistance. In the absence of GIP receptor, fat is not efficiently accumulated in adipocytes, but is used predominantly as the preferred energy source.

Here, we have shown that the GIP receptor expressed in pancreatic β-cells contributes to meal-induced insulin secretion, espe-

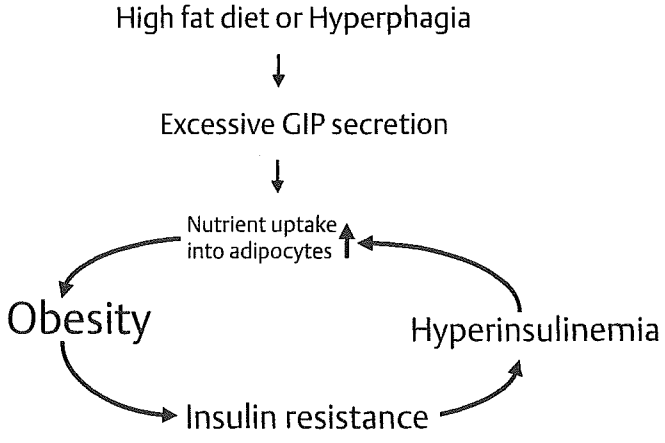

Fig. **3** GIP links excessive intake of nutrients to obesity. See text in detail.

cially in the early phase; we have also shown that the GIP receptor expressed in adipocytes contributes to nutrient uptake into adipocytes. Expression of GIP receptor other than in pancreatic β-cells and adipocytes has been demonstrated. The physiological significance of GIP will be uncovered after full characterization of the GIP receptor KO mice.

Acknowledgements

This study was supported in part by Grants-in-Aid for Scientific Research from the Ministry of Education, Culture, Sports, Science and Technology, Japan.

References

[1] Perley MJ, Kipnis DM. Plasma insulin responses to oral and intravenous glucose: studies in normal and diabetic subjects. J Clin Invest 1967; 46: 1954 – 1962

[2] Creutzfeldt W. The incretin concept today. Diabetologia 1979; 16: 75 – 85

[3] Pederson RA, Schubert HE, Brown JC. The insulinotropic action of gastric inhibitory polypeptide. Can J Physiol Pharmacol 1975; 53: 217 – 223

[4] Yamada Y, Hayami T, Nakamura K, Kaisaki PJ, Someya Y, Wang CZ, Seino S, Seino Y. Human gastric inhibitory polypeptide receptor: cloning of the gene (GIPR) and cDNA. Genomics 1995; 29: 773 – 776

[5] Usdin TB, Mezey E, Button DC, Brownstein MJ, Bonner TI. Gastric inhibitory polypeptide receptor, a member of the secretin-vasoactive intestinal peptide receptor family, is widely distributed in peripheral organs and the brain. Endocrinology 1993; 133: 2861 – 2870

[6] Miyawaki K, Yamada Y, Yano H, Niwa H, Ban N, Ihara Y, Kubota A, Fujimoto S, Kajikawa M, Kuroe A, Tsuda K, Hashimoto H, Yamashita T, Jomori T, Tashiro F, Miyazaki J, Seino Y. Glucose intolerance caused by a defect in the entero-insular axis: a study in gastric inhibitory polypeptide receptor knockout mice. Proc Natl Acad Sci USA 1999; 96: 14843 – 14847

[7] Miyawaki K, Yamada Y, Ban N, Ihara Y, Tsukiyama K, Zhou H, Fujimoto S, Oku A, Tsuda K, Toyokuni S, Hiai H, Mizunoya W, Fushiki T, Holst JJ, Makino M, Tashita A, Kobara Y, Tsubamoto Y, Jinnouchi T, Jomori T, Seino Y. Inhibition of gastric inhibitory polypeptide signaling prevents obesity. Nat Med 2002; 8: 738 – 742

[8] Pamir N, Lynn FC, Buchan AM, Ehses J, Hinke SA, Pospisilik JA, Miyawaki K, Yamada Y, Seino Y, McIntosh CH, Pederson RA. Glucose-dependent insulinotropic polypeptide receptor null mice exhibit compensatory changes in the enteroinsular axis. Am J Physiol 2003; 284: E931 – 939

[9] Hansotia T, Baggio LL, Delmeire D, Hinke SA, Yamada Y, Tsukiyama K, Seino Y, Holst JJ, Schuit F, Drucker DJ. Double incretin receptor knockout (DIRKO) mice reveal an essential role for the enteroinsular axis in transducing the glucoregulatory actions of DPP-IV inhibitors. Diabetes 2004; 53: 1326 – 1335

[10] Preitner F, Ibberson M, Franklin I, Binnert C, Pende M, Gjinovci A, Hansotia T, Drucker DJ, Wollheim C, Burcelin R, Thorens B. Gluco-incretins control insulin secretion at multiple levels as revealed in mice lacking GLP-1 and GIP receptors. J Clin Invest 2004; 113: 635 – 645

[11] Tsukiyama K, Yamada Y, Miyawaki K, Hamasaki A, Nagashima K, Hosokawa M, Fujimoto S, Takahashi A, Toyoda K, Toyokuni S, Oiso Y, Seino Y. Gastric inhibitory polypeptide is the major insulinotropic factor in K_{ATP} null mice. Eur J Endocrinol 2004; 151: 407 – 412

[12] Miki T, Nagashima K, Tashiro F, Kotake K, Yoshitomi H, Tamamoto A, Gonoi T, Iwanaga T, Miyazaki J, Seino S. Defective insulin secretion and enhanced insulin action in KATP channel-deficient mice. Proc Natl Acad Sci USA 1998; 95: 10402 – 10406

[13] Creutzfeldt W, Ebert R, Willms B, Frerichs H, Brown JC. Gastric inhibitory polypeptide (GIP) and insulin in obesity: increased response to stimulation and defective feedback control of serum levels. Diabetologia 1978; 14: 15 – 24

[14] Flatt PR, Bailey CJ, Kwasowski P, Swanston-Flatt SK, Marks V. Abnormalities of GIP in spontaneous syndromes of obesity and diabetes in mice. Diabetes 1983; 32: 433 – 435

[15] Yip RG, Boylan MO, Kieffer TJ, Wolfe MM. Functional GIP receptors are present on adipocytes. Endocrinology 1998; 139: 4004 – 4007

[16] Eckel RH, Fujimoto WY, Brunzell JD. Gastric inhibitory polypeptide enhanced lipoprotein lipase activity in cultured preadipocytes. Diabetes 1979; 28: 1141 – 1142

Am J Physiol Endocrinol Metab 284: E931–E939, 2003.
First published January 21, 2003; 10.1152/ajpendo.00270.2002.

Glucose-dependent insulinotropic polypeptide receptor null mice exhibit compensatory changes in the enteroinsular axis

Nathalie Pamir,[1] Francis C. Lynn,[1] Alison M. J. Buchan,[1] Jan Ehses,[1] Simon A. Hinke,[1] J. Andrew Pospisilik,[1] Kazumasa Miyawaki,[2] Yuichiro Yamada,[2] Yutaka Seino,[2] Christopher H. S. McIntosh,[1] and Raymond A. Pederson[1]

[1]*Department of Physiology, University of British Columbia, Vancouver, British Columbia, Canada, V6T 1Z3; and* [2]*Department of Metabolism and Clinical Nutrition, Graduate School of Medicine, Kyoto University, Kyoto 606-8507, Japan*

Submitted 19 June 2002; accepted in final form 18 January 2003

Pamir, Nathalie, Francis C. Lynn, Alison M. J. Buchan, Jan Ehses, Simon A. Hinke, J. Andrew Pospisilik, Kazumasa Miyawaki, Yuichiro Yamada, Yutaka Seino, Christopher H. S. McIntosh, and Raymond A. Pederson. Glucose-dependent insulinotropic polypeptide receptor null mice exhibit compensatory changes in the enteroinsular axis. *Am J Physiol Endocrinol Metab* 284: E931–E939, 2003. First published January 21, 2003; 10.1152/ajpendo.00270.2002.—The incretins glucose-dependent insulinotropic polypeptide (GIP) and glucagon-like peptide-1 (GLP-1) are gut hormones that act via the enteroinsular axis to potentiate insulin secretion from the pancreas in a glucose-dependent manner. Both GLP-1 receptor and GIP receptor knockout mice (*GLP-1R*$^{-/-}$ and *GIPR*$^{-/-}$, respectively) have been generated to investigate the physiological importance of this axis. Although reduced GIP action is a component of type 2 diabetes, GIPR-deficient mice exhibit only moderately impaired glucose tolerance. The present study was directed at investigating possible compensatory mechanisms that take place within the enteroinsular axis in the absence of GIP action. Although serum total GLP-1 levels in GIPR knockout mice were unaltered, insulin responses to GLP-1 from pancreas perfusions and static islet incubations were significantly greater (40–60%) in *GIPR*$^{-/-}$ than in wild-type (*GIPR*$^{+/+}$) mice. Furthermore, GLP-1-induced cAMP production was also elevated twofold in the islets of the knockout animals. Pancreatic insulin content and gene expression were reduced in *GIPR*$^{-/-}$ mice compared with *GIPR*$^{+/+}$ mice. Paradoxically, immunocytochemical studies showed a significant increase in β-cell area in the GIPR-null mice but with less intense staining for insulin. In conclusion, *GIPR*$^{-/-}$ mice exhibit altered islet structure and topography and increased islet sensitivity to GLP-1 despite a decrease in pancreatic insulin content and gene expression.

insulin; GLP-1; pancreas perfusion; cAMP; incretin

THE TERM ENTEROINSULAR AXIS was first proposed by Unger and Eisentraut (42) to describe the nutrient, neural, and endocrine interactions between the gut and the endocrine pancreas that amplify insulin secretion. The increased insulin release in response to oral glucose vs. intravenous administration is called the incretin effect. The two most important incretins that act via the enteroinsular axis are glucose-dependent insulinotropic polypeptide [GIP-(1–42)] and truncated forms of glucagon-like peptide-1 (GLP-1): GLP-1-(7–36NH_2) and GLP-1-(7–37) (15, 34).

These peptides account for nearly 50% of postprandial insulin release and therefore play a major role in glucose homeostasis (30). The insulinotropic effects of GIP and GLP-1 are transduced through specific G protein-coupled receptors on the β-cell, resulting in stimulation of adenylyl cyclase (5, 46) and phospholipase A_2 (9) and increased levels of intracellular Ca^{2+} (20, 25). In addition to their insulinotropic effects, both incretins stimulate insulin gene expression and biosynthesis in the β-cell (5, 11). Non-β-cell-mediated effects of GLP-1, including inhibition of gastric emptying and glucagon secretion, also contribute to its blood glucose-lowering effects (3, 47). The possible involvement of GIP and GLP-1 in the etiology of diabetes is still controversial. Studies have shown that, although GIP action is diminished, GLP-1 activity is preserved in type 2 diabetes (28, 29). A recent study from Lynn et al. (24) linked decreased GIP action to reduced GIP receptor levels in the Vancouver Diabetic Zucker (VDF) animal model of type 2 diabetes. Although GLP-1 secretion has been reported to be normal (13, 29, 44), increased (16, 32), or decreased (43) in type 2 diabetes due to its preserved insulinotropic activity in the diabetic state, GLP-1 has been widely studied as a possible therapeutic agent (17).

The relative contribution of the incretins to the enteroinsular axis is still under investigation. Mice that are deficient in functional GIP or GLP-1 receptors (*GIPR*$^{-/-}$ and *GLP-1R*$^{-/-}$ mice, respectively) provide unique models for the study of incretin physiology. Both mouse models have impaired glucose tolerance but normal feeding behavior and body weight (26, 37). Different fasting plasma glucose levels have been reported in different colonies. We report that the *GLP-1R*$^{-/-}$ colony exhibits normal glucose levels, whereas others have reported increased fasting levels (33, 37).

Address for reprint requests and other correspondence: Raymond A. Pederson, Dept. of Physiology, Faculty of Medicine, Univ. of British Columbia, 2146 Health Sciences Mall, Vancouver, BC, Canada V6T 1Z3 (E-mail: pederson@interchange.ubc.ca).

The costs of publication of this article were defrayed in part by the payment of page charges. The article must therefore be hereby marked "*advertisement*" in accordance with 18 U.S.C. Section 1734 solely to indicate this fact.

In addition, *GLP-1R*$^{-/-}$ mice have elevated plasma GIP levels and increased β-cell sensitivity to GIP, demonstrating that disruption of one component of the enteroinsular axis may be compensated for by another (33). We hypothesized that this compensatory mechanism is due to a physiological balance between the incretins, allowing for maintenance of glucose homeostasis, and that a similar compensation (enhanced GLP-1/insulin axis) would be observed in the *GIPR*$^{-/-}$ mouse. In the present study, we have tested this hypothesis and report that the sensitivity of the β-cell to GLP-1 is indeed enhanced in the *GIPR*$^{-/-}$ mouse along with reduced pancreatic insulin content and altered islet topography.

MATERIALS AND METHODS

Animals. The background and generation of GIPR-deficient C57BL/6 mice used in this study have been previously described (26). All animal experiments were performed in accordance with the guidelines put forth by the University of British Columbia Committee on Animal Care and the Canadian Council on Animal Care. For all the experiments, only 9- to 14-wk-old male *GIPR*$^{-/-}$ and C57BL/6 control mice were used.

Oral glucose tolerance test and hormone radioimmunoassays. After an overnight fast, control and *GIPR*$^{-/-}$ mice were administered 1 g/kg glucose (as a 10% solution) via gavage. Blood glucose levels were measured individually for each mouse by use of a handheld glucometer (Surestep; Lifescan, Burnaby, BC, Canada). Because only a limited volume of blood could be removed from each mouse and it was necessary to measure plasma GIP, GLP-1, and insulin levels in each sample, blood from 5–6 animals was pooled at $t = 0$ and $t = 20$ min after an oral glucose tolerance test (OGTT). Plasma was then separated by centrifugation at 12,000 *g* for 15 min at 4°C and stored at −20°C until hormone radioimmunoassay (RIA). The GIP RIA utilized a COOH-terminally directed antibody (rabbit anti-human) that has been extensively used for measuring total GIP immunoreactivity [GIP-(1–42) and GIP-(3–42)] (33). Total GLP-1 concentrations were measured by using the rat total GLP-1 kit from Linco (St. Charles, MO) as directed by the manufacturer. The GLP-1 antibody recognizes total immunoreactive GLP-1 (GLP-1-(7–36NH_2), GLP-1-(7–37), and NH_2-terminally truncated forms) and has a detection limit of 3 pM. Insulin was assayed by using a sensitive rat insulin kit (Linco) with an antibody that cross-reacts 100% with mouse insulin. Plasma dipeptidyl peptidase IV (DP IV) activity (μU/ml) was measured colorimetrically (405 nm) through enzymatic release of *p*-nitroanilide (*p*-NA) from H-gly-pro-*p*-NA (35).

Insulin tolerance test. *GIPR*$^{+/+}$ and *GIPR*$^{-/-}$ mice were fasted for 3 h and given 0.01 U/g insulin (Humulin R, 100 U/ml; Lilly, Toronto, ON, Canada) by intraperitoneal injection. Blood glucose was measured with a handheld glucometer.

In vitro perfused pancreas. *GIPR*$^{+/+}$ and *GIPR*$^{-/-}$ mice were fasted overnight and anesthetized by intraperitoneal injection of 80 mg/kg pentobarbital sodium (Somnotol; MTC Pharmaceuticals, Cambridge, ON, Canada) before surgery. The surgical procedure and the pancreas perfusion protocol are described in Pederson et al. (33). Briefly, the abdominal aorta and the portal vein were cannulated with PE-50 tubing (Cole-Palmer, Chicago, IL). The perfusate consisted of a Krebs-Ringer bicarbonate buffer supplemented with 3% dextran (Sigma, Oakville, ON, Canada) and 0.2% bovine serum albumin (BSA, fraction V, RIA grade; Sigma) gassed with 5% CO_2 to achieve and maintain pH 7.4. The flow rate was maintained at 1 ml/min, and the outflow was collected at 1-min intervals. GIP and GLP-1 (both from Probiodrug, Hala, Germany) were delivered by sidearm infusion in the presence of 16.7 mM glucose, resulting in a 1 nM final concentration, whereas arginine (10 mM; Sigma) was mixed directly into the perfusate containing 8.8 mM glucose. Insulin was measured by RIA as previously described (33).

Isolation and culture of pancreatic islets. Fed mice were anesthetized with Somnotol, and islets of Langerhans were isolated by collagenase digestion. Collagenase (type V, 2 mg/ml; Sigma) in Hanks' balanced salt solution (HBSS; GIBCO-Life Technologies, Burlington, ON, Canada) supplemented with 10 mM HEPES (GIBCO), 2 mM L-glutamine (Sigma), and 0.2% BSA was injected into the common bile duct to inflate the pancreas. The pancreas was then removed and digested at 37°C for 10 min. The pancreas was then dispersed mechanically with a siliconized Pasteur pipette, washed, filtered through a 1-mm nylon screen, and washed again. Islets were separated by centrifugation at 1,800 *g* for 20 min in a discontinuous dextran gradient. Hand-picked islets were cultured overnight in RPMI 1640 (Sigma) with 8.8 mM glucose, 10% fetal calf serum (Cansera, Rexdale, ON, Canada), 50 U/ml each of penicillin G (Sigma) and streptomycin (Sigma), 0.07% human serum albumin (Sigma), 0.0025% human apotransferrin (GIBCO), 25 pM sodium selenite (VWR, Mississauga, ON, Canada) and 10 μM ethanolamine (VWR).

Islet cAMP and insulin measurements. After overnight culture, 15–18 healthy islets were selected, washed twice with 0.5 ml of Krebs-Ringer supplemented with 0.2% BSA and 4.4 mM glucose, and incubated at 37°C for 30 min. Thereafter, islets were incubated in the presence or absence of 10 nM GIP or GLP-1 or 10 μM forskolin (Sigma) in the same buffer with 0.5 mM 3-isobutyl-1-methylxanthine (Research Biochemicals International, Natick, MA) and 16.7 mM glucose. After a 30-min incubation, islets were lysed by boiling for 3 min in 0.05 N HCl. Samples were subsequently dried by vacuum centrifugation (Speed-Vac; Sorvall, Farmingdale, NY) and stored at −20°C. cAMP levels were assayed by using a kit according to the manufacturer's instructions (Biomedical Technologies, Stoughton, MA). For insulin measurements, islets were collected after overnight culture, washed twice with Krebs-Ringer, and incubated for 45 min in 4.4 mM glucose containing Krebs-Ringer supplemented with 0.1% BSA. After a short centrifugation, the medium was replaced with either 16.7 mM glucose alone or 16.7 mM glucose plus 10 nM GIP or GLP-1. After 45 min, islets were lysed by boiling for 5 min in 1 M acetic acid and centrifuged, and supernatants were assayed for insulin (24).

Measurement of pancreatic insulin content. Animals were rendered unconscious with CO_2 and exsanguinated. Pancreata were removed, homogenized in 2 M acetic acid, and then boiled for 5 min. Homogenates were centrifuged at 15,000 *g* for 15 min, and the supernatant was stored at −70°C. Total protein levels were measured with a bicinchoninic acid kit (Pierce, Rockford, IL), and insulin values (measured as described) were normalized to total protein content (ng/μg protein) (33).

Isolation and measurement of islet insulin and GLP-1 receptor mRNA by reverse transcriptase real-time polymerase chain reaction (PCR). Freshly isolated islets were washed twice with HBSS and solubilized in 1 ml TRIzol (GIBCO) and kept at −70°C. After isolation, 50 ng of total RNA were subjected to reverse transcription (RT) in a volume of 10 μl containing 0.5 mM deoxynucleotide triphosphates, 15 pmol

specific primers targeted at the carboxy termini of the mouse GLP-1 receptor open reading frame (5′-ACC AAC AGG GAG GAC CGG-3′) or the mouse insulin II gene (5′-GTA GTT CTC CAG CTG GTA GAG GG-3′) 100 U Superscript II RNAse H$^-$ reverse transcriptase (GIBCO), 10 U RNAse inhibitor (RNA Guard; Amersham Pharmacia, Piscataway, NJ), 1 mM dithiothreitol, 50 mM Tris·HCl (pH 8.3), 75 mM KCl, and 3 mM $MgCl_2$. After RT, 10 ng (2 μl) of mouse cDNA were used in the real-time PCR reaction to measure insulin and GLP-1 receptor expression. The PCR reaction mix consisted of 1× TaqMan Buffer A (PE Applied Biosystems, Foster City, CA), 10 mM $MgCl_2$, 200 μM each dATP, dCTP, and dGTP, 400 μM dUTP, 200 nM mouse GLP-1 receptor 5′ forward primer (5′-CAG GGC TTG ATG GTG GCT ATC-3′) or mouse insulin II 5′ forward primer (5′-TGG AGG CCC GGG AGC-3′), 200 nM mouse GLP-1 receptor 3′ reverse primer (5′-CGC TCC CAG CAT TTC CG-3′) or mouse insulin II 3′ reverse primer (5′-ATC TAC AAT GCC ACG CTT CTG C-3′), and 100 nM GLP-1 receptor probe colabeled with the fluorescent dyes VIC and 6-carboxy-tetramethylrhodamine (TAMRA) (5′-ACT GCT TTG TCA ACA ATG AGG TCC AGA TGG-3′) or insulin II probe colabeled with fluorescent dyes TET and TAMRA (5′-ACC TTC AGA CCT TGG CAC TGG AGG TG-3′), 0.01 U/μl AmpErase-uracil *N*-glycosylase (UNG; PE Applied Biosystems), and 0.025 U/μl AmpliTaq Gold (PE Applied Biosystems). PCR reactions were carried out in triplicate in the PE Applied Biosystems 7700 sequence detection system. The reaction profile included a 10-min preincubation at 50°C to allow the UNG to degrade any uracil-containing nucleic acids and a further 10-min incubation at 94°C to activate the AmpliTaq Gold. After these preincubations, a two-step PCR protocol was carried out, which included a denaturation step at 94°C for 15 s followed by a 1-min annealing/extension step at 60°C. Fluorescence was measured during the annealing/extension steps over 40 cycles and used to calculate a cycle threshold (Ct), i.e., the point at which the reaction is in the exponential phase and is detectable by the hardware. All reactions followed the typical sigmoidal reaction profile, and Ct was used as a measure of amplicon abundance (12). The results were normalized over total wild-type mRNA levels.

Immunocytochemistry. Mice were fasted overnight before being killed. Pancreata from wild-type and knockout mice (n = 5 each) were fixed separately in Bouin's solution (75% picric acid, 8% formaldehyde, 5% glacial acetic acid) for 1 h at room temperature and washed thoroughly with 70% ethanol. The tissue was embedded in paraffin wax, and three consecutive 5-μm sections were taken 300 μm apart and mounted on glass slides. The study was carried out blind: slides were coded to prevent identification of +/+ and −/− tissues before quantification. The sections were dewaxed in xylene and cleared in petroleum ether (Sigma). The sections were then rehydrated in PBS (80 mM Na_2HPO_4, 1.47 mM KH_2PO_4, 2.86 mM KCl, 137 mM NaCl). To control for intra-immunostain variability, all of the sections were incubated in the same batch of solutions and stained simultaneously. The β-cells were detected by overnight incubation with a polyclonal rabbit anti-mouse insulin antibody (1:100, Santa Cruz Biotechnologies, Santa Cruz, CA), followed by a 90-min incubation with a biotinylated goat anti-rabbit secondary antibody (1:300, Jackson Labs, West Grove, PA) at room temperature. Sections were then washed and incubated with avidin-biotin peroxidase complex (Vector Labs, Burlington, ON, Canada) at a dilution of 1:1,000 in PBS supplemented with 5% horse serum (Sigma). The peroxidase reaction was developed with 2% diaminobenzidine tetrahydrochloride in 0.05 M Tris (pH 7.5) with 0.2% H_2O_2. After being counterstained with hematoxylin for 5 min, the sections were dehydrated through graded alcohol, and coverslips were applied with Permount (Fisher Scientific, Nepean, ON, Canada). The sections were analyzed using the NIH Image software (http://rsb.info.nih.gov/nih-image/), and data were analyzed as islet area over total pancreatic area. Five separate fields of view (under ×10 magnification) per section were randomly chosen, the periphery of the islets in this area was outlined, and area was determined by using the analysis software. The islet area from the five random samples was then normalized to the total pancreatic area in those five fields. Once the quantification had been completed, the source of the sections (*GIPR*$^{+/+}$ or *GIPR*$^{-/-}$) was identified and statistical significance was assessed.

Data analysis. All data are expressed as means ± SE. An unpaired Student's t-test and a Mann-Whitney U-test (exclusively for immunocytochemistry) were used to compare the control values with *GIPR*$^{-/-}$ mouse values, where $P < 0.05$ was considered statistically significant. The data analysis and area under the curve calculations were carried out by using graphic analysis software (Graphpad, Prism, San Diego, CA).

RESULTS

OGTT. The OGTT profile of *GIPR*$^{-/-}$ mice over 120 min is very similar to that of the wild-type control animals (Fig. 1*A*). The 15- and 30-min blood glucose were moderately (18%) but significantly greater in *GIPR*$^{-/-}$ mice. To allow for concurrent measurement of insulin and incretin levels, basal and 20-min blood samples from another OGTT were pooled. This time point was chosen on the basis of preliminary studies to achieve near-peak incretin levels (data not shown). Fasting glucose and insulin levels were both comparable in *GIPR*$^{-/-}$ and wild-type mice (Fig. 1, *B* and *C*). However, after a glucose challenge, the 20-min plasma glucose levels were significantly higher in *GIPR*$^{-/-}$ mice than in wild-type mice ($P < 0.05$), and insulin levels were 45% lower in *GIPR*$^{-/-}$ mice than in wild-type mice (Fig. 1, *B* and *C*). To further assess the hormonal components of the enteroinsular axis in *GIPR*$^{-/-}$ mice, fasting and 20-min total plasma immunoreactive GLP-1 and immunoreactive GIP levels were determined (Fig. 1, *D* and *E*). Total GLP-1 levels did not differ in *GIPR*$^{-/-}$ mice compared with wild-type (Fig. 1*D*, $P > 0.05$). However, fasting plasma GIP levels were elevated, whereas the 20-min levels were lowered by 25% in *GIPR*$^{-/-}$ compared with *GIPR*$^{+/+}$ mice (Fig. 1*E*, $P < 0.05$). Plasma DP IV activity was unaltered between groups: values for fasting were 10.5 ± 0.9 vs. 10.2 ± 0.8 μU/ml and 9.1 ± 1.5 vs. 8.7 ± 0.6 μU/ml for 20-min in *GIPR*$^{+/+}$ and *GIPR*$^{-/-}$ mice, respectively.

To explain the alterations in plasma GIP levels, the duodeno-jejunal GIP content was also measured in fed mice. A reduction of 15% in *GIPR*$^{-/-}$ mice was observed compared with control animals (67.5 ± 8.2 pg/ml, n = 6, in *GIPR*$^{+/+}$ vs. 59.7 ± 4.8 pg/ml, n = 7, in *GIPR*$^{-/-}$ mice, $P < 0.05$).

Insulin tolerance test. To investigate the insulin sensitivity of the *GIPR*$^{-/-}$ mice, blood glucose levels were determined after an insulin challenge. Blood glucose profile over 1 h did not differ in *GIPR*$^{-/-}$ mice compared with wild-type control mice (Fig. 2).

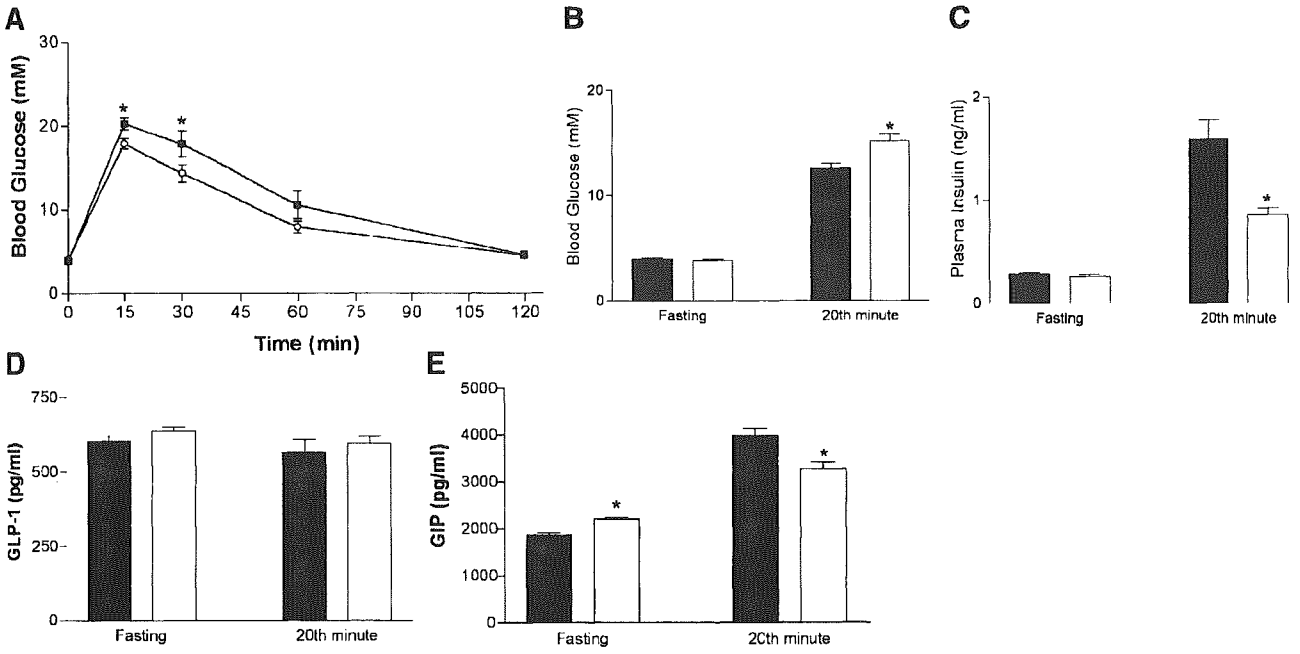

Fig. 1. Oral glucose tolerance test (OGTT) and fasting and 20th-min OGTT plasma total immunoreactive (ir) glucagon-like peptide (GLP)-1, and glucose-dependent insulinotropic polypeptide (GIP) levels in wild-type (WT) and *GIPR*$^{-/-}$ mice. *A*: blood glucose levels in WT (○, $n = 7$) and *GIPR*$^{-/-}$ (■, $n = 11$) mice during an OGTT. *B*: blood glucose levels for fasting and 20th min of an OGTT in WT (filled bars, $n = 21$) and *GIPR*$^{-/-}$ (empty bars, $n = 23$) animals. *C*: plasma fasting and 20th-min insulin levels in WT (filled bars, $n = 4$, pooled from 21 animals) and *GIPR*$^{-/-}$ (empty bars, $n = 4$, pooled from 23 animals). Plasma total irGLP-1 (*D*) and irGIP (*E*) levels in WT and *GIPR*$^{-/-}$. Values are means ± SE (*$P < 0.05$).

In vitro insulin responses to GIP, glucose, arginine, and GLP-1. To verify that GIP was unable to stimulate insulin secretion from the pancreata of *GIPR*$^{-/-}$ animals, in vitro perfusions were carried out (Fig. 3*A*). As expected, 1 nM GIP generated no insulin response from the perfused knockout pancreata. Subsequently, low (4.4 mM) and high (16.7 mM) glucose perfusions were also performed, demonstrating that glucose-stimulated insulin secretions in *GIPR*$^{-/-}$ and wild-type mice were comparable (Fig. 3*B*). In type 2 diabetic patients, insulin responses to secretagogues such as high glucose, sulfonylurea, and arginine are blunted (45). To assess the insulin response of *GIPR*$^{-/-}$ islets to a stimulant other than glucose, high-dose arginine (10 mM) perfusions were performed in the presence of 8.8 mM glucose (Fig. 3*C*). The results showed no significant differences in insulin secretion between *GIPR*$^{-/-}$ and control animals. However, *GIPR*$^{-/-}$ mice exhibited a higher peak and sustained insulin release in response to GLP-1 perfusion (Fig. 3*D*). The integrated insulin response to perfusion with 1 nM GLP-1 was 60% greater in *GIPR*$^{-/-}$ mice compared with wild-type mice (Fig. 3*E*). To determine whether these results were due to an inherent change in islet physiology, islets were isolated, cultured overnight, and stimulated with low (4.4 mM) and high (16.7 mM) glucose alone or in the presence of either 10 nM GIP or GLP-1 (Fig. 4*A*). The insulin secreted over 45 min was 40% greater in response to GLP-1 stimulation for *GIPR*$^{-/-}$ vs. *GIPR*$^{+/+}$ islets ($P < 0.05$), consistent with the data from perfusion experiments. Additionally, GIP did not stimulate insulin release from *GIPR*$^{-/-}$ islets, and the insulin response to 16.7 mM glucose was comparable in both groups.

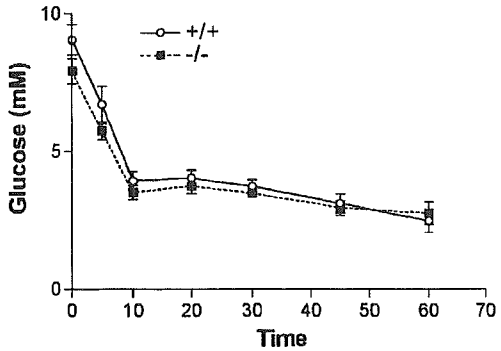

Fig. 2. Insulin tolerance test. Blood glucose was measured after insulin challenge in WT control (+/+; ○, $n = 8$) and in *GIPR*$^{-/-}$ (−/−; ■, $n = 8$) mice. Values are means ± SE.

Intracellular cAMP production in isolated islets. To correlate GLP-1-stimulated insulin release with receptor activation, we measured cAMP production in response to GLP-1 in isolated islets (Fig. 4*B*). Forskolin was used as a positive control to assess maximal cAMP production and thus allow normalization of responses to account for discrepancies in islet size and number. Interestingly, basal (16.7 mM glucose) cAMP levels

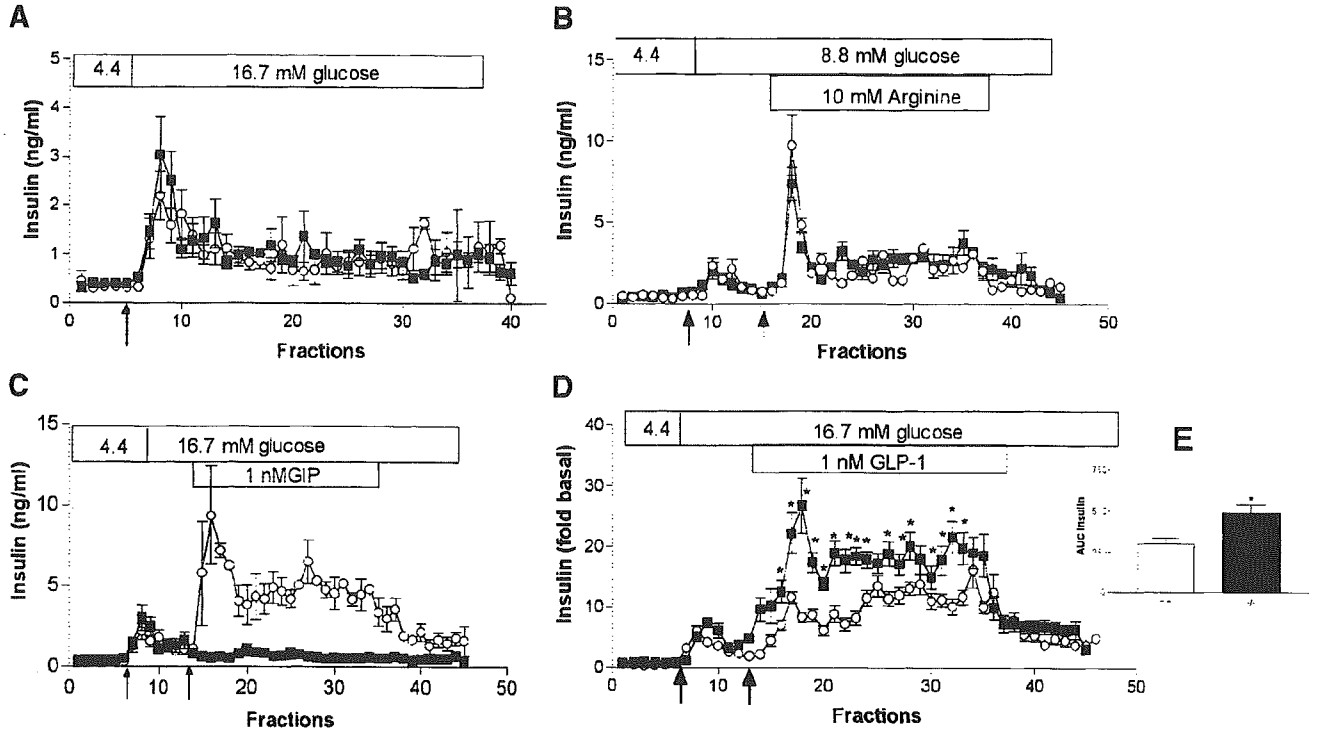

Fig. 3. Insulin secretion from perfused pancreas in response to GIP, glucose alone, arginine, and GLP-1 in WT and *GIPR*$^{-/-}$ mice. Insulin secretion from the perfused pancreas in response to: 1 nM GIP in WT control (○, $n = 3$) and *GIPR*$^{-/-}$ (■, $n = 4$) mice (*A*); 4.4 and 16.7 mM glucose in WT control and *GIPR*$^{-/-}$ mice ($n = 4$; *B*); and 10 mM arginine in WT control and *GIPR*$^{-/-}$ mice ($n = 4$; *C*). *D*: 1 nM GLP-1, presented as fold of basal, in control and *GIPR*$^{-/-}$ mice ($n = 6$). *E*: mean integrated insulin response for *GIPR*$^{+/+}$ and *GIPR*$^{-/-}$ mice (*$P < 0.05$). AUC, area under the curve. Arrows indicate switching between conditions. Values are means ± SE.

were significantly increased in *GIPR*$^{-/-}$ mice compared with wild-type mice. GLP-1-stimulated cAMP production was also significantly increased in *GIPR*$^{-/-}$ animals vs. wild-type mice ($P < 0.05$), implying that β-cell sensitivity to GLP-1 was increased. Thus these findings are also consistent with the perfusion and static islet stimulation experiments.

Pancreatic insulin content and islet insulin and GLP-1 mRNA content. Both GIP and GLP-1 stimulate insulin gene transcription and protein synthesis in the β-cell (11). Thus absence of GIP action may lead to alterations in insulin gene transcription and, therefore, pancreatic insulin content. The total insulin content from fed mice pancreata was significantly lower (~40%) in *GIPR*$^{-/-}$ than in *GIPR*$^{+/+}$ mice (Fig. 6*A*; $P < 0.05$). Furthermore, these data are supported by the finding that insulin mRNA levels were significantly reduced (~40%) in isolated islets of *GIPR*$^{-/-}$ mice compared with controls (Fig. 5*A*, $P < 0.05$). Finally, assessment of GLP-1 receptor mRNA levels revealed that, despite an increase in GLP-1 sensitivity, there was no increase in GLP-1 receptor mRNA levels in the islets of *GIPR*$^{-/-}$ mice (Fig. 5*B*).

Immunocytochemistry. Immunocytochemical studies were carried out to assess the effect of GIP receptor deficiency on islet and pancreas morphology. β-Cell area as a percentage of total pancreatic area was significantly increased (~45%) in knockout vs. wild-type mice (Fig. 6*B*; $P < 0.05$). Additionally, when stained under identical experimental conditions, the staining intensity for insulin was reduced in *GIPR*$^{-/-}$ islets (Fig. 6, *C* and *D*). The whole pancreas weight was not different between groups: 1.6 ± 0.4 vs. 1.7 ± 0.3 g in *GIPR*$^{+/+}$ and *GIPR*$^{-/-}$, respectively.

DISCUSSION

The reduced effect of GIP on insulin secretion in type 2 diabetic patients has been described (21, 29). It has been suggested that this might be due to reduced receptor expression in the β-cell, resulting in its lowered sensitivity to GIP (18). Recently, this possibility was addressed in a model of type 2 diabetes, the VDF rat, in which it was demonstrated that GIP receptor expression was reduced (24). Therefore, mice with a targeted disruption of the GIPR gene (*GIPR*$^{-/-}$) may provide a useful model for studying the potential implications of a lack of GIP signaling on glucose homeostasis and the development of type 2 diabetes. Miyawaki et al. (26) have shown that these mice exhibit modest glucose intolerance along with a 50% reduction in insulin secretion in response to oral glucose, whereas weight gain was reported to remain unchanged under both normal and high-fat diet conditions. It was the hypothesis of the present study that these mice would exhibit compensatory

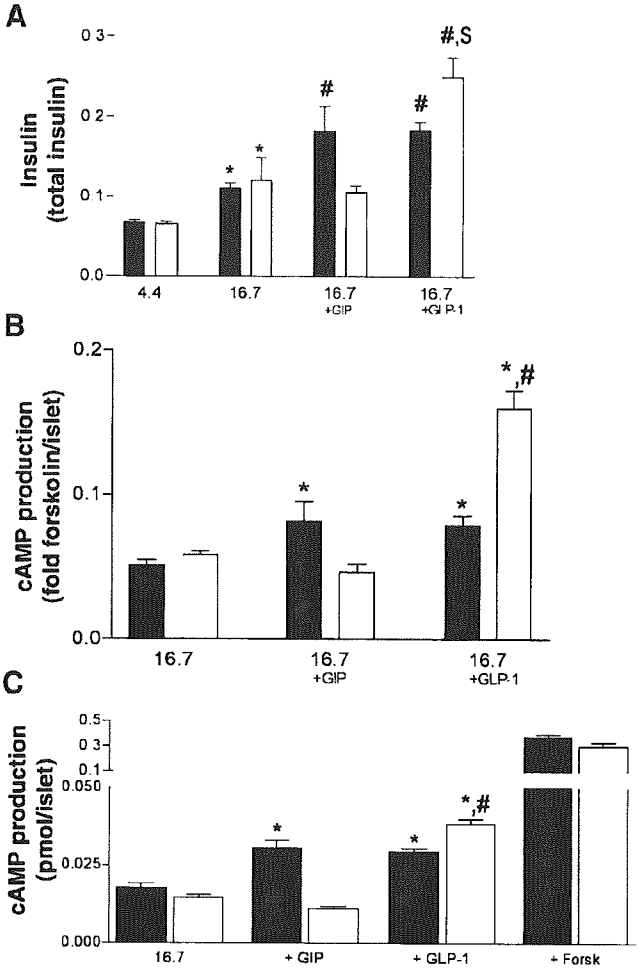

Fig. 4. Static stimulation of isolated pancreatic islets from WT and *GIPR*$^{-/-}$ mice. *A*: insulin secretion in response to GIP (n = 4) and GLP-1 (n = 6) in WT control (filled bars) and *GIPR*$^{-/-}$ (empty bars) mice. ($\$P < 0.05$ WT vs. *GIPR*$^{-/-}$; $*P < 0.05$ 16.7 vs. 4.4 mM glucose; $\#P < 0.05$ vs. 16.7 mM glucose alone). Values are means ± SE. *B*: cAMP production in response to GIP and GLP-1 stimulation in isolated islets from WT control (filled bars) and *GIPR*$^{-/-}$ (empty bars) mice. Data have been normalized to forskolin and are presented as %forskolin. *C*: cAMP production presented with the real values without normalization to forskolin. For all conditions, n = 5–8; $\#P < 0.05$ WT vs. *GIPR*$^{-/-}$; $*P < 0.05$: vs. basal. Values are means ± SE.

changes in the enteroinsular axis to overcome the absence of GIP action.

Immunoneutralization studies examining the relative contribution of GIP to the enteroinsular axis were first reported in the early 1980s (6–8). In more recent studies, the treatment of rats with a GIP antagonist, GIP-(7–30NH$_2$), has been shown to result in a 72% decrease in postprandial insulin release along with normal glucose levels (40). Later, the same group provided evidence that GIP-(7–30NH$_2$) inhibits glucose transport from the small intestine, which might in part explain the relatively small rise in serum glucose levels after oral glucose despite a profound decrease in postprandial insulin levels (41). Studies using a GIPR antibody have suggested that GIP acts as an anticipatory signal to the β-cell to potentiate insulin release, which in turn primes the periphery for glucose disposal (22). The same antibody was used on *GLP-1R*$^{-/-}$ and *GLP-1R*$^{+/+}$ mice, and it was concluded by Baggio et al. (2) that GIP had a restricted role in the regulation of glucose homeostasis. These studies involved relatively short-term antagonist administration and therefore may not be reflective of the consequences of the chronic absence of the GIP action. The use of GIPR-null mice provides a new approach to the investigation of the effects of GIP.

Despite the loss of GIP receptors, the 2-h blood glucose profiles for *GIPR*$^{-/-}$ and wild-type mice are remarkably similar (Fig. 1*A*). Blood glucose reached peak values for both groups of animals at the 15-min time point, and the curves merged after 40 min. The subtle increase (18%) in plasma glucose levels at the 20th min of the OGTT does not correlate with the more profound reduction (55%) in plasma insulin levels in the *GIPR*$^{-/-}$ animals (Fig. 1, *B* and *C*), suggesting a possible change in insulin sensitivity or glucose disposal. Controversy exists as to whether GLP-1 is capable of exerting insulin-like effects on peripheral tissue in addition to the well-studied insulinotropic effects. Studies have shown that GLP-1 improves glucose disposal in type 2 diabetes by enhancing insulin-stimulated glucose utilization (36), and these effects have been shown to be independent of the amount of insulin secreted (4, 14). Recently, Ahren and Pacini (1) re-

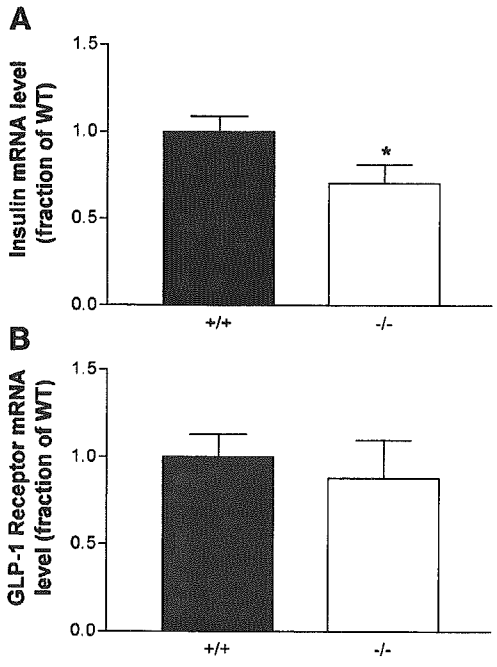

Fig. 5. Isolated pancreatic islet insulin and GLP-1 receptor mRNA content. *A*: islet insulin mRNA levels in *GIPR*$^{+/+}$ (filled bars, n = 10) and *GIPR*$^{-/-}$ (empty bars, n = 9) mice. *B*: islet GLP-1 receptor mRNA levels in *GIPR*$^{+/+}$ (n = 12) and *GIPR*$^{-/-}$ (n = 12). Values are presented relative to WT mRNA represented as 1.0 and are means ± SE ($*P < 0.05$).

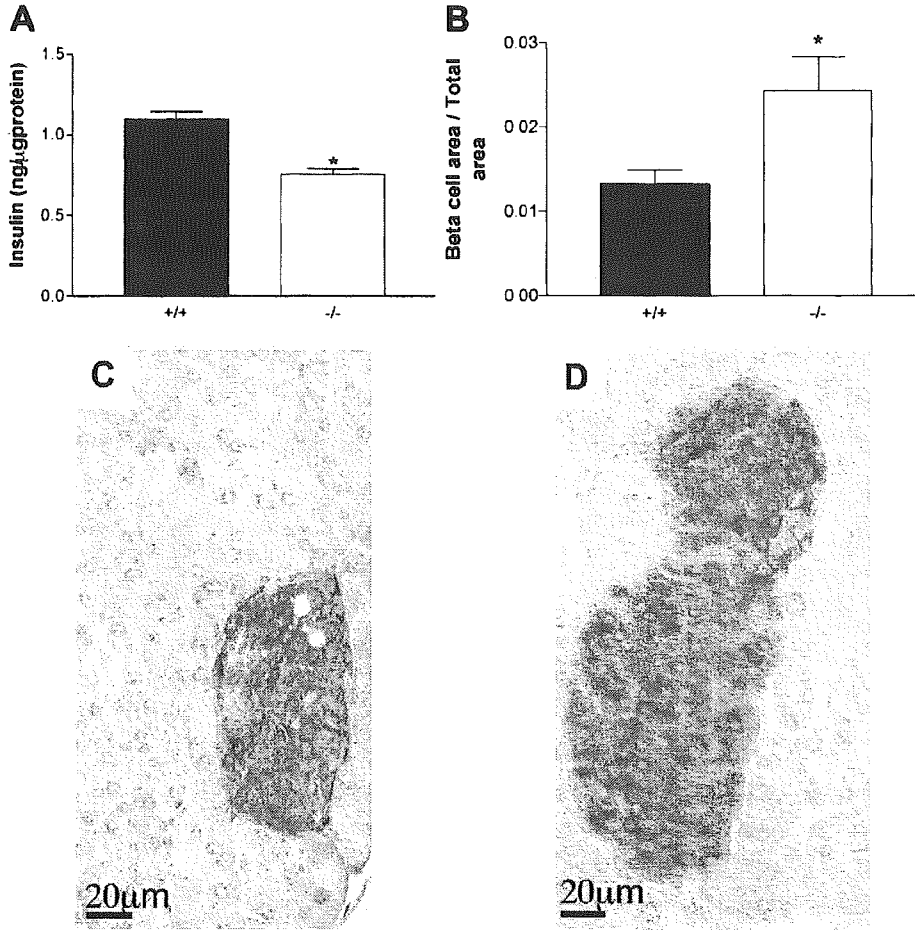

Fig. 6. Total pancreatic insulin content and pancreatic β-cell area. *A*: total pancreatic insulin content in fed *GIPR*$^{+/+}$ (filled bars, n = 5) and *GIPR*$^{-/-}$ (empty bars, n = 5) mice. Insulin content was normalized for total protein content. *B*: relative area occupied by β-cells (fold total area) in *GIPR*$^{+/+}$ and *GIPR*$^{-/-}$ mice (*P < 0.05). Peroxidase staining for insulin in *GIPR*$^{+/+}$ (*C*) and *GIPR*$^{-/-}$ mice (*D*) shows that the area occupied by the β-cells in the *GIPR*$^{+/+}$ mice is smaller than in *GIPR*$^{-/-}$ mice.

ported that, in mice, the effects of GLP-1 on glucose homeostasis were mainly insulin mediated and the use of a relatively specific GLP-1 receptor antagonist, exendin-(9–39), reversed these actions. It remains unclear whether an increased extrapancreatic sensitivity to GLP-1 might play a role in the alteration in glucose clearance in *GIPR*$^{-/-}$ mice. We report normal sensitivity to insulin in GIPR$^{-/-}$ mice (Fig. 2); therefore, it appears that enhanced GLP-1 action is not insulin mediated. However, GLP-1 is able to potentiate insulin action (36), and it is possible that, in *GIPR*$^{-/-}$ mice, enhanced GLP-1 action ameliorates insulin action. Furthermore, it is also possible that, in these mice, the enhanced glucose disposal (relative to the insulin levels present) could be a result of the delayed gastric emptying (caused by GLP-1) (31) due to increased peripheral tissue GLP-1 sensitivity.

Similar to *GIPR*$^{-/-}$ mice, *GLP-1R*$^{-/-}$ mice have been shown to exhibit modest glucose intolerance, with upregulation, in this case, of the GIP component of the enteroinsular axis (33). The present study was designed in part to test whether the converse was true in *GIPR*$^{-/-}$ animals. Miyawaki et al. (26) showed that, when administered an intraperitoneal glucose challenge (thus bypassing the enteroinsular axis), *GIPR*$^{-/-}$ mice exhibited no alteration in glucose disposal relative to wild-type animals. In the present study, pancreas perfusion (Fig. 3), static islet stimulation (Fig. 4*A*), and cAMP production (Fig. 4*B*) data clearly showed that the GLP-1 component of the enteroinsular axis in *GIPR*$^{-/-}$ mice was upregulated. These data agree with the evidenced alteration in oral glucose tolerance in the face of unchanged intraperitoneal glucose tolerance. The combined findings that in vitro insulin responses to high glucose and arginine are similar and that islet GLP-1 receptor mRNA levels in *GIPR*$^{-/-}$ and in *GIPR*$^{+/+}$ mice are comparable suggest that compensation occurs distally to the GLP-1 receptor on the β-cell. Because both incretins act through G protein-coupled receptors and signal via the adenylyl cyclase-cAMP system (5, 27, 46), it could be hypothesized that the permanent absence of GIP receptors leads to a compensatory increase in coupling efficiency of GLP-1 receptors. Although the GLP-1 receptor mRNA levels are comparable, we do not have information about the protein synthesis. Hence, despite similar gene expression, the protein synthesis might be enhanced, leading to increased sensitivity to GLP-1. The possibility of upregulation of GLP-1 secretion appears unlikely, since no changes in GLP-1 levels were observed 20 min after an oral glucose challenge (Fig. 1*D*), nor were there changes in activity of plasma DP IV, the primary

inactivating enzyme for GIP and GLP-1 (35). Together these data suggest that the majority of the compensatory changes in the GLP-1 axis of *GIPR*$^{-/-}$ mice lay at a postreceptor level in the β-cell. That said, the observed reduction in circulating insulin levels and modest increase in blood glucose show that compensation by the GLP-1 axis is not complete and that, although the functions of GIP and GLP-1 overlap, both are required for proper glycemic control.

GIPR$^{-/-}$ mice were shown to have a 40% reduction in pancreatic insulin content and gene expression concomitant with a twofold increase in β-cell area (Fig. 6, *A* and *B*), suggesting that insulin gene expression and content were reduced in the GIPR-null mice on a cellular level. Because both GIP and GLP-1 stimulate insulin gene expression (5, 11), it might be predicted that an increase in β-cell GLP-1 sensitivity in the absence of GIP action could protect against a decrease in islet insulin mRNA and protein levels. The decrease in insulin mRNA and protein synthesis in *GIPR*$^{-/-}$ mice is comparable to the 35% decrease that was shown by Pederson et al. (33) in *GLP-1R*$^{-/-}$ mice. Hence, absence of either of the incretins results in abnormalities within the β-cell, leading to impaired insulin content. Thus the compensation by GLP-1 or by GIP at the β-cell level, in *GIPR*$^{-/-}$ and in *GLP-1R*$^{-/-}$ mice, respectively, seems not to extend as far as insulin biosynthesis.

In addition to stimulation of insulin production on the cellular level, GLP-1 has also been shown to be involved in the morphological development of the islets of Langherhans. In immunocytochemical studies, Ling et al. (23) showed α- and δ-cell migration toward the islet core and a reduction in islet size in *GLP-1R*$^{-/-}$ mouse pancreata. Examination of pancreatic sections from *GIPR*$^{-/-}$ mice with the same objective showed no such changes in endocrine cell distribution, only in β-cell area (Fig. 6). Reduced insulin gene expression and insulin content correlated well with less intensely stained islets in *GIPR*$^{-/-}$ mice (Fig. 6). Immunostaining for glucagon and somatostatin showed normal topology and distribution with no indication of migration toward the islet core (data not shown). Very recently, it has been shown that GLP-1 has growth hormone-like effects on pancreatic islets and on β-cells (19). Thus the enhanced GLP-1 action on the *GIPR*$^{-/-}$ mouse pancreas, indicated by pancreas perfusions and static islet stimulation, was consistent with the observed increase in β-cell area. Recently, studies have shown on βTC3 insulin-secreting tumors that GIP is a regulator of upstream kinases of apoptosis cascades. In this regard, our finding of increased β-cell area in *GIPR*$^{-/-}$ mice is not fully understood (10, 38, 39). Further studies are required to examine the role of GIP on islet growth and insulin gene expression to clarify these findings. To date, there have been no conclusive studies that have examined the effects of GIP on islet/β-cell development and survival in vivo.

In summary, we have demonstrated that disruption of the GIP component of the enteroinsular axis in mice results in decreased insulin gene transcription and protein biosynthesis, increased islet sensitivity to GLP-1, and changes in islet structure. We report that compensation for the absence of a functional GIP receptor occurs, in part, by upregulation of the GLP-1 component of the enteroinsular axis. The physiological changes that take place in both the *GIPR*$^{-/-}$ and the *GLP-1R*$^{-/-}$ strains of knockout mice suggest that the incretins act in concert to maintain glucose homeostasis and that a balance between the two is required for proper function of the enteroinsular axis. Further experiments, targeted at clarifying the molecular changes that occur within the β-cell, are required to extend our understanding of GIP physiology.

Technical assistance was provided by Cuilan Nian.

This work was supported by the Canadian Institutes for Health Research Grant 590007, and the Canada Foundation for Innovation.

REFERENCES

1. **Ahren B and Pacini G.** Dose-related effects of GLP-1 on insulin secretion, insulin sensitivity, and glucose effectiveness in mice. *Am J Physiol Endocrinol Metab* 277: E996–E1004, 1999.
2. **Baggio L, Kieffer TJ, and Drucker DJ.** Glucagon-like peptide-1, but not glucose-dependent insulinotropic peptide, regulates fasting glycemia and nonenteral glucose clearance in mice. *Endocrinology* 141: 3703–3709, 2000.
3. **Creutzfeldt WOC, Orskov C, Kleine N, Holst JJ, Willms B, and Nauck MA.** Glucagonostatic actions and reduction of fasting hyperglycemia by exogenous glucagon-like peptide-1 (7–36) amide in type 1 diabetic patients. *Diabetes Care* 19: 580–586, 1996.
4. **D'Alessio DA, Prigeon RL, and Ensinck JW.** Enteral enhancement of glucose disposition by both insulin- dependent and isulin-independent process—a physiological role of glucagon-like peptide 1. *Diabetes* 44: 1433–1437, 1995.
5. **Drucker DJ, Philippe J, Mojsov S, Chick WL, and Habener JF.** Glucagon-like peptide I stimulates insulin gene expression and increases cAMP levels in a rat islet cell line. *Proc Natl Acad Sci USA* 84: 3434–3438, 1987.
6. **Ebert R and Creutzfeldt W.** Influence of gastric inhibitory polypeptide antiserum on glucose-induced insulin secretion in rats. *Endocrinology* 111: 1601–1606, 1982.
7. **Ebert R, Illmer K, and Creutzfeldt W.** Release of gastric inhibitory polypeptide (GIP) by intraduodenal acidification in rats and humans and abolishment of the incretin effect of acid by GIP-antiserum in rats. *Gastroenterology* 76: 515–523, 1979.
8. **Ebert R, Unger H, and Creutzfeldt W.** Preservation of incretin activity after removal of gastric inhibitory polypeptide (GIP) from rat gut extracts by immunoadsorption. *Diabetologia* 24: 449–454, 1983.
9. **Ehses JA, Lee SST, Pederson RA, and McIntosh CHS.** A new pathway for glucose-dependent insulinotropic polypeptide (GIP) receptor signaling—evidence for the involvement of phospholipase A, in GIP-stimulated insulin secretion. *J Biol Chem* 276: 23667–23673, 2001.
10. **Ehses JA, Pelech SL, Pederson RA, and McIntosh CH.** Glucose-dependent insulinotropic polypeptide activates the Raf-Mek1/2-ERK1/2 module via a cyclic AMP/cAMP-dependent protein kinase/Rap1-mediated pathway. *J Biol Chem* 277: 37088–37097, 2002.
11. **Fehmann HC, Gherzi R, and Goke B.** Regulation of islet hormone gene expression by incretin hormones. *Exp Clin Endocrinol Diabetes* 103: 56–65, 1995.
12. **Freeman WM, Walker SJ, and Vrana KE.** Quantitative RT-PCR: pitfalls and potential. *Biotechniques* 26: 112–125, 1999.
13. **Greenbaum C, Prigeon R, and D'Alessio D.** Impaired β-cell function, incretin effect, and glucagon suppression in patients with type 1 diabetes who have normal fasting glucose. *Diabetes* 51: 951–957, 2002.
14. **Gutniak MK, Svartberg J, Hellstrom PM, Holst JJ, Adner N, and Ahren B.** Antidiabetogenic action of glucagon-like pep-

tide-1 related to administration relative to meal intake in subjects with type 2 diabetes. *J Intern Med* 250: 81–87, 2001.
15. **Habener JF.** The incretin notion and its relevance to diabetes. *Endocrinol Metab Clin North Am* 22: 775–794, 1993.
16. **Hiroyoshi M, Tateishi K, Yasunami Y, Maeshiro K, Ono J, Matsuoka Y, and Ikeda S.** Elevated plasma levels of glucagon-like peptide-1 after oral glucose ingestion in patients with pancreatic diabetes. *Am J Gastroenterol* 94: 976–981, 1999.
17. **Holst JJ.** Glucagon-like peptide-1, a gastrointestinal hormone with a pharmaceutical potential. *Curr Med Chem* 6: 1005–1017, 1999.
18. **Holst JJ, Gromada J, and Nauck MA.** The pathogenesis of NIDDM involves a defective expression of the GIP receptor. *Diabetologia* 40: 984–986, 1997.
19. **Holz GG and Leech CA.** Glucagon-like peptide-1: an insulinotropic hormone with potent growth factor actions at the pancreatic islets of Langerhans. *Molecular Basis of Pancreas Development and Function*, edited by Habener JF and Hussain MA. Norwell, MA: Kluwer Academic, 2001, p. 109–141.
20. **Kieffer TJ and Habener JF.** The glucagon-like peptides. *Endocr Rev* 20: 876–913, 1999.
21. **Krarup T, Saurbrey N, Moody AJ, Kuhl C, and Madsbad S.** Effect of porcine gastric inhibitory polypeptide on β-cell function in type I and type II diabetes mellitus. *Metabolism* 36: 677–682, 1984.
22. **Lewis JT, Dayanandan B, Habener JF, and Kieffer TJ.** Glucose-dependent insulinotropic polypeptide confers early phase insulin release to oral glucose in rats: demonstration by a receptor antagonist. *Endocrinology* 141: 3710–3716, 2000.
23. **Ling Z, Wu D, Zambre Y, Flamez D, Drucker DJ, Pipeleers DG, and Schuit FC.** Glucagon-like peptide 1 receptor signaling influences topography of islet cells in mice. *Virchows Arch* 438: 382–387, 2001.
24. **Lynn FC, Pamir N, Ng EHC, McIntosh CHS, Kieffer TJ, and Pederson RA.** Defective glucose-dependent insulinotropic polypeptide receptor expression in diabetic fatty Zucker rats. *Diabetes* 50: 1004–1011, 2001.
25. **McIntosh CH, Wheeler MB, Gelling RW, Brown JC, and Pederson RA.** GIP receptors and signal-transduction mechanisms. *Acta Physiol Scand* 157: 361–365, 1996.
26. **Miyawaki K, Yamada Y, Yano H, Niwa H, Ban N, Ihara Y, Kubota A, Fujimoto S, Kajikawa M, Kuroe A, Tsuda K, Hashimoto H, Yamashita T, Jomori T, Tashiro F, Miyazaki J, and Seino Y.** Glucose intolerance caused by a defect in the entero-insular axis: a study in gastric inhibitory polypeptide receptor knockout mice. *Proc Natl Acad Sci USA* 96: 14843–14847, 1999.
27. **Moens K, Heimberg H, Flamez D, Huypens P, Quartier E, Ling Z, Pipeleers D, Gremlich S, Thorens B, and Schuit F.** Expression and functional activity of glucagon, glucagon-like peptide I, and glucose-dependent insulinotropic peptide receptors in rat pancreatic islet cells. *Diabetes* 45: 257–261, 1996.
28. **Nauck M, Stockmann F, Ebert R, and Creutzfeldt W.** Reduced incretin effect in type 2 (non-insulin-dependent) diabetes. *Diabetologia* 29: 46–52, 1986.
29. **Nauck MA, Heimesaat MM, Orskov C, Holst JJ, Ebert R, and Creutzfeldt W.** Preserved incretin activity of glucagon-like peptide 1 [7–36 amide] but not of synthetic human gastric inhibitory polypeptide in patients with type-2 diabetes mellitus. *J Clin Invest* 91: 301–307, 1993.
30. **Nauck MA, Homberger E, Siegel EG, Allen RC, Eaton RP, Ebert R, and Creutzfeldt W.** Incretin effects of increasing glucose loads in man calculated from venous insulin and C-peptide responses. *J Clin Endocrinol Metab* 63: 492–498, 1986.
31. **Nauck MA, Niedereichholz U, Ettler R, Holst JJ, Orskov C, Ritzel R, and Schmiegel WH.** Glucagon-like peptide 1 inhibition of gastric emptying outweighs its insulinotropic effects in healthy humans. *Am J Physiol Endocrinol Metab* 273: E981–E988, 1997.
32. **Orskov C, Jeppesen J, Madsbad S, and Holst JJ.** Proglucagon products in plasma of noninsulin-dependent diabetics and nondiabetic controls in the fasting state and after oral glucose and intravenous arginine. *J Clin Invest* 87: 415–423, 1991.
33. **Pederson RA, Satkunarajah M, McIntosh CHS, Scrocchi LA, Flamez D, Schuit F, Drucker DJ, and Wheeler MB.** Enhanced glucose-dependent insulinotropic polypeptide secretion and insulinotropic action in glucagon-like peptide 1 receptor (−/−) mice. *Diabetes* 47: 1046–1052, 1998.
34. **Pederson RA, Schubert HE, and Brown JC.** The insulinotropic action of gastric inhibitory polypeptide. *Can J Physiol Pharmacol* 53: 217–223, 1975.
35. **Pospisilik JA, Stafford SG, Demuth H-U, Brownsey R, Parkhouse W, Finegood DT, McIntosh CHS, and Pederson RA.** Long-term treatment with dipeptidyl peptidase IV inhibitor P32/98 causes sustained improvements in glucose tolerance, insulin sensitivity, hyperinsulinemia, and beta cell glucose responsiveness in VDF (fa/fa) Zucker rats. *Diabetes* 51: 943–950, 2002.
36. **Sandhu H, Wiesenthal SR, MacDonald PE, McCall RH, Tchipashvili V, Rashid S, Satkunarajah M, Irwin DM, Shi ZQ, Brubaker PL, Wheeler MB, Vranic M, Efendic S, and Giacca A.** Glucagon-like peptide 1 increases insulin sensitivity in depancreatized dogs. *Diabetes* 48: 1045–1053, 1999.
37. **Scrocchi LA, Brown TJ, Maclusky N, Brubaker PL, Auerbach AB, Joyner AL, and Drucker DJ.** Glucose intolerance but normal satiety in mice with null mutation in the glucagon-like peptide 1 receptor gene. *Nat Med* 2: 1254–1258, 1996.
38. **Trumper A, Trumper K, and Horsch D.** Mechanisms of mitogenic and anti-apoptotic signaling by glucose-dependent insulinotropic polypeptide in β(INS-1)-cells. *J Endocrinol* 174: 233–246, 2002.
39. **Trumper A, Trumper K, Trusheim H, Arnold R, Goke B, and Horsch D.** Glucose-dependent insulinotropic polypeptide is a growth factor for β (INS-1) cells by pleiotropic signaling. *Mol Endocrinol* 15: 1559–1570, 2001.
40. **Tseng CC, Kieffer TJ, Jarboe LA, Usdin TB, and Wolfe MM.** Postprandial stimulation of insulin release by glucose-dependent insulinotropic polypeptide (GIP). Effect of a specific glucose-dependent insulinotropic polypeptide receptor antagonist in the rat. *J Clin Invest* 98: 2440–2445, 1996.
41. **Tseng CC, Zhang XY, and Wolfe MM.** Effect of GIP and GLP-1 antagonists on insulin release in the rat. *Am J Physiol Endocrinol Metab* 276: E1049–E1054, 1999.
42. **Unger RH and Eisentraut AM.** Entero-insular axis. *Arch Intern Med* 123: 261–266, 1969.
43. **Vaag A, Holst J, Volund A, and Beck-Nielsen H.** Gut incretin hormones in identical twins discordant for non-insulin-dependent diabetes mellitus (NIDDM)—evidence for decreased glucagon-like peptide 1 secretion during oral glucose ingestion in NIDDM twins. *Eur J Endocrinol* 135: 425–432, 1996.
44. **Vilsboll T, Krarup T, Madsbad S, and Holst J.** Defective amplification of the late phase insulin response to glucose by GIP in obese type II diabetic patients. *Diabetologia* 45: 1111–1119, 2002.
45. **Ward WK, Beard JC, and Porte DJ.** Clinical aspects of islet β cell function in non-insulin-dependent diabetes mellitus. *Diabetes Metab Res Rev* 2: 297–312, 1986.
46. **Wheeler MB, Gelling RW, McIntosh CH, Georgiou J, Brown JC, and Pederson RA.** Functional expression of the rat pancreatic islet glucose-dependent insulinotropic polypeptide receptor: ligand binding and intracellular signaling properties. *Endocrinology* 136: 4629–4639, 1995.
47. **Willms B, Werner J, Holst JJ, Orskov C, Creutzfeldt W, and Nauck MA.** Gastric empying glucose responses, and insulin secretion after a liquid test meal—effects of exogenous glucagon-like peptide-1 (GLP-1)-(7–36) amide in type 2 (noninsulin dependent) diabetic patients. *J Clin Endocrinol Metab* 81: 327–332, 1996.

Porphyromonas Gingivalis Infection Is Associated With Carotid Atherosclerosis in Non-Obese Japanese Type 2 Diabetic Patients

Ataru Taniguchi, Fusanori Nishimura, Yoji Murayama, Shoichiro Nagasaka, Mitsuo Fukushima, Masahiko Sakai, Satoru Yoshii, Akira Kuroe, Haruhiko Suzuki, Yoshihiro Iwamoto, Yoshihiko Soga, Takahide Okumura, Masahito Ogura, Yuichiro Yamada, Yutaka Seino, and Yoshikatsu Nakai

The aim of the present study was to investigate whether non-obese Japanese type 2 diabetic patients with porphyromonas gingivalis infection have atherosclerotic vascular diseases. A total of 134 non-obese Japanese type 2 diabetic patients (96 men and 38 women, aged 36 to 84 years, body mass index [BMI] 20.1 to 26.9 kg/m^2) were studied. In conjunction with BMI, glycosylated hemoglobin (HbA_{1c}), fasting glucose, and serum lipids (triglycerides, total cholesterol, high-density lipoprotein [HDL] cholesterol, low-density lipoprotein [LDL] cholesterol) were measured. LDL cholesterol was calculated using the Friedewald formula. Using high-resolution B-mode ultrasound scan, we measured intimal medial thickness (IMT) in plaque-free segments of bilateral common carotid arteries, and the mean of IMT in 2 vessels was used for the analysis. Furthermore, we calculated the degree of stenosis in plaque segments of bilateral common carotid arteries. The degree of carotid atherosclerosis was expressed as a percentage ratio between the area of plaque and that of the lumen using the formula (Lumen Area Residual − Lumen Area)/Lumem Area × 100. Both the areas were automatically measured by the system on a frozen transverse scanning plane at the site of maximal narrowing. When 2 or more plaques were present in the vessel, only that causing the greatest degree of stenosis was considered for analysis. Values represent mean±SEM unless otherwise stated. Immunoglobulin G (IgG) titer against porphyromonas gingivalis was 245 ± 65 (mean ± 2 SD) in nondiabetic healthy subjects. In contrast, there was a wide variation in IgG titer against porphyromonas gingivalis in type 2 diabetic patients studied (range, 16 to 26,800). Thus, we classified our type 2 diabetic patients into 2 subpopulations according to the value of mean ± 2 SD (= 310) of nondiabetic healthy subjects: one with high IgG titer against porphyromonas gingivalis (>310) (1,422 ± 408) and the other with normal IgG titer against porphyromonas gingivalis (<310) (152 ± 10, P = .002). The populations did not differ with respect to age, sex, BMI, fasting glucose, HbA_{1c}, serum triglycerides, total, HDL, and LDL cholesterol levels. Although the mean IMT in plaque-free segments was not different between the 2 groups (0.73 ±0.03 *v* 0.68 ± 0.02 mm, P = .098), the degree of stenosis in plaque segments was significantly higher in the high IgG titer group (12.0% ± 2.2%) than in normal one (5.5% ± 1.4%, P = .009). From these results, it can be concluded that porphyromonas gingivalis infection, although still a subclinical infection, is associated with atherosclerotic vascular disease in non-obese Japanese type 2 diabetic patients.

THE MAJOR CLINICAL consequence of type 2 diabetes is mortality and morbidity from atherosclerotic vascular disease. Regarding the risk factors responsible for the evolution of atherosclerosis in diabetic patients, Bierman[1] previously estimated that typical risk factors including smoking, cholesterol, and blood pressure (BP) can account for no more than 25% to 30% of excess cardiovascular risk factors in diabetic patients. This suggests that other factors might play a key role in the progression of atherosclerosis in diabetes. The degree of atherosclerosis can be evaluated by high-resolution B-mode ultrasound scan. Carotid atherosclerosis is important in view of its relationship to cerebrovascular ischemic diseases and coronary atherosclerosis.[2]

Whereas insulin resistance is established to be one of the risk factors for the evolution of coronary heart disease (CHD),[3] there are some data suggesting that subclinical inflammation is hypothesized to be associated with CHD events in man.[4-7] Elevated levels of C-reactive protein (CRP), although still for the most part in the healthy reference range, have been shown to be associated with increased risk of future CHD events.[4-6] Some cross-sectional and case-control studies have reported elevated antibody titers directed against Chlamydia pneumoniae, Helicobacter pyroli, and Cytomegalovirus among those with prevalent heart disease.[7]

Type 2 diabetic patients are known to have a high prevalence of atherosclerosis and periodontal disease.[8] Porphyromonas gingivalis has been shown to play an important role in the periodontis of type 2 diabetic patients.[9] Thus, periodontis especially porphyromonas gingivalis infection is hypothesized to be associated with atherosclerosis in type 2 diabetic patients. To the best of our knowledge, however, the relationship between porphyromonas gingivalis infection and the degree of atherosclerosis has not been fully clarified in type 2 diabetic patients. In this regard, a major problem is that the degree of being overweight or of hyperglycemia per se affects atherosclerosis in man. To overcome this difficulty, we recruited non-obese well-controlled unique Japanese type 2 diabetic patients who had no evidence of cardiovascular disease, ischemic

From the Division of Diabetes, Kansai-Denryoku Hospital, Osaka; Department of Patho-physiology/Periodontal Science, Okayama University Graduate School of Medicine and Dentistry, Okayama; Division of Endocrinology and Metabolism, Jichi Medical School, Tochigi; and the Department of Metabolism and Clinical Nutrition, Graduate School of Medicine and College of Medical Technology, Kyoto University, Kyoto, Japan.

Submitted January 14, 2002; accepted July 30, 2002.

Address reprint requests to Ataru Taniguchi, MD, Division of Diabetes, Kansai-Denryoku Hospital, 2-1-7 Fukushima, Fukushima-ku, Osaka-City, Osaka 553-0003, Japan.

0026-0495/03/5202-0040$35.00/0
doi:10.1053/meta.2003.50001

stroke, or chronic renal failure and investigated the relationships between porphyromonas gingivalis infection and the degree of carotid atherosclerosis. This is the first description that porphyromonas gingivalils infection is associated with carotid atherosclerosis in non-obese Japanese type 2 diabetic patients.

SUBJECTS AND METHODS

One hundred and 34 non-obese Japanese type 2 diabetic patients who visited Kansai-Denryoku Hospital were enrolled for the present study. Type 2 diabetes mellitus was diagnosed based on the criteria of the World Health Organization (WHO).[10] They had no evidence of current acute illness including clinically significant infectious disease. The duration of diabetes was 11.2 ± 0.7 years (mean ± SEM). Ninty-three of 134 diabetic patients were taking sulfonylureas (gliclazide) to control their diabetes and the rest with diet alone. None of the patients have received insulin therapy. All subjects had ingested at least 150 g of carbohydrates for the 3 days preceding the study. None of the subjects had significant renal, hepatic, or cardiovascular disease. They did not consume alcohol or perform heavy exercise for at least 1 week before the study.

The blood was drawn in the morning after a 12-hour fast. Plasma glucose was measured with the glucose oxidase method. Triglycerides, total and high-density lipoprotein (HDL) cholesterol were measured. The low-density lipoprotein (LDL) cholesterol was calculated using the Friedewald formula.[11]

Serum immunoglobulin G (IgG) antibody titer against porphyromonas gingivalis was assayed by enzyme-linked immunosorbent assay as described previously.[12] Porphyromonas gingivalis SU 83 was used as an antigen. A soluble fraction of whole bacterial sonicates was used as an antigen and was prepared as described previously.[12]

A carotid sonography was performed with high-resolution B-mode scanning equipment (Logic 500 GE Yokogawa, Milwaukee, WI) with a 7.5-MHz sector scanner probe.[13] The common carotid arteries of both sides were examined with longitudinal and transverse scans, because we could not analyze the internal and external carotid arteries fully in all patients. The coefficient of variation (CV) for interobserver variability was found to be 8.5% and the CV for intraobserver variability was 6.0%. The intimal plus medial thickness (IMT) of the common carotid artery was measured in plaque-free segments as the distance from the leading edge of the first echogenic line to that of the second echogenic line. The mean of IMT in plaque-free segments of bilateral common carotid arteries was used for the analysis. The degree of stenosis was also measured in the plaque segments of bilateral common carotid arteries. It was calculated as a percentage ratio between the area of the plaque and that of the lumen using the formula (Lumen Area − Residual Lumen Area)/Lumen Area × 100. Both the areas were automatically measured by the system on a frozen transverse scanning plane at the site of maximal narrowing. When 2 or more plaques were present in the vessel, only that causing the greatest degree of stenosis was considered for analysis.

Statistical Analysis

The statistical analysis was performed with the StatView 5 system (Statview, Berkeley, CA). The differences of mean were determined by the Student's t test, taking a value of $P < .05$ as significant. Data were expressed as the mean ± SEM unless otherwise stated.

RESULTS

The subjects studied were all Japanese type 2 diabetic patients (96 men and 38 women) with an age range of 36 to 84 years (60.8 ± 0.8) and a body mass index (BMI) of 20.1 to 26.9 kg/m^2 (23.3 ± 0.2). They were all non-obese.[14] The fasting plasma glucose was 147 ± 3 mg/dL and glycosylated hemoglobin (HbA_{1c}) was 7.1% ± 0.1%. Serum triglycerides, total, and HDL cholesterol levels were 129 ± 7 mg/dL and 203 ± 3 mg/dL, and 52 ± 1 mg/dL, respectively. Serum LDL concentration was 125 ± 3 mg/dL. Mean IMT in plaque-free segments was 0.71 ± 0.02 mm. In contrast, the degree of carotid stenosis in plaque segments was 8.9% ± 1.4%.

Table 1. Clinical Characteristics in High and Normal IgG Titer Against Porphyromonas Gingivalis

Characteristic	High Titer	Normal Titer	*P*
Antibody titers	>310	<310	—
Antibody titers	1,422 ± 408	152 ± 10	.002
No. of subjects studied	70	64	—
Male/Female	48/22	48/16	.056
Degree of carotid stenosis (%)	12.0 ± 2.2	5.5 ± 1.4	.009
Mean IMT (mm)	0.73 ± 0.03	0.68 ± 0.02	.098
Triglycerides (mg/dL)	130 ± 9	127 ± 10	.393
Total cholesterol (mg/dL)	206 ± 4	200 ± 4	.148
LDL cholesterol (mg/dL)	128 ± 3	121 ± 5	.100
HDL cholesterol (mg/dL)	51 ± 2	53 ± 2	.234
BMI (kg/m^2)	23.3 ± 0.2	23.3 ± 0.2	.475
Fasting glucose (mg/dL)	148 ± 4	147 ± 5	.452
HbA_{1c} (%)	7.2 ± 0.1	7.4 ± 0.2	.198
Age (yr)	62 ± 1	60 ± 1	.150
Systolic blood pressure	129 ± 2	131 ± 2	.253
Diastolic blood pressure	75 ± 1	76 ± 1	.247

IgG titer against porphyromonas gingivalis was 245 ± 65 (mean ± 2 SD) in nondiabetic healthy subjects. In contrast, there was a wide variation in IgG titer against porphyromonas gingivalis in type 2 diabetic patients studied (range, 16 to 26,800). Thus, we classified our type 2 diabetic patients into 2 subpopulations according to the value of mean ± 2 SD of nondiabetic healthy subjects (= 310): one with a high IgG titer against porphyromonas gingivalis (> 310) (1,422 ± 408) and the other with a normal IgG titer against porphyromonas gingivalis (< 310) (152 ±10, $P = .002$). There was no overlap in IgG titer between the 2 populations. Seventy-one percent (50/70) of the patients with a high titer and 68% (43/64) of those with a normal titer were treated with sulfonylurea. The rests were treated with diet alone. No significant difference was observed in medication status between the 2 groups. When the patients were divided into high and normal IgG titer subgroups, the degree of carotid stenosis was significantly higher in high titer subgroups than in normal titer subgroups (12.0% ± 2.2% *v* 5.5% ± 1.4%, $P = .009$). The mean IMT in plaque-free segments was higher in the high IgG titer group than in the normal one, but was not statistically significant (0.73 ± 0.03 *v* 0.68 ± 0.02 mm, $P = .098$). Serum triglycerides, total, and LDL cholesterol levels were higher in the patients with a high IgG titer than in those with a normal IgG titer, but they were not statistically significant between the 2 groups. No significant difference was observed in HDL cholesterol, BMI, fasting glucose, HbA_{1c}, age, and systolic and diastolic BP between the 2 subgroups (Table 1).

DISCUSSION

Our main observation in the present study is that 70 of 134 patients (52%) had high IgG titer against porphyromonas gin-